

## REPORT DOCUMENTATION

AD-A261 230

Approved  
No 0704-0188

Public reporting burden for this collection of information is estimated to average 1 hour per response, including the time for reviewing existing data sources, gathering and maintaining the data needed, and completing and reviewing the collection of information, including suggestions for reducing this burden. To A Davis Highway, Suite 1204 Arlington, VA 22202-4302 and to the Office of Man-



Archiving existing data sources, or any other aspect of this and Reports, 1215 Jefferson Ave, DC 20503

1. AGENCY USE ONLY (Leave blank)		2. REPORT DATE 2/15/93		Interim June 1, 1990 to February 1993	
4. TITLE AND SUBTITLE Intramolecular Bridge/Terminal Oxo Exchange within [MoV <sub>2</sub> O <sub>3</sub> ] <sup>4+</sup> Complexes Containing Linear Oxo Bridges				5. FUNDING NUMBERS C: N00014-90-J-1762 R and T Code: 4135025	
6. AUTHOR(S) Robert L. Thompson, Samkeun Lee, Steven J. Geib and N. John Cooper					
7. PERFORMING ORGANIZATION NAME(S) AND ADDRESS(ES) Department of Chemistry University of Pittsburgh Pittsburgh, PA 15260				8. PERFORMING ORGANIZATION REPORT NUMBER --	
9. SPONSORING/MONITORING AGENCY NAME(S) AND ADDRESS(ES) Department of the Navy Office of the Chief of Naval Research Arlington, VA 22217-5000				10. SPONSORING/MONITORING AGENCY REPORT NUMBER	
11. SUPPLEMENTARY NOTES Submitted for publication in the Journal of American Chemical Society					
12a. DISTRIBUTION/AVAILABILITY STATEMENT This document has been approved for public release and sale; its distribution is unlimited.				12b. DISTRIBUTION CODE --	
13. ABSTRACT (Maximum 200 words)  See attached  <div style="text-align: center;"><b>DTIC</b> <b>SELECTED</b> <b>FEB 24 1993</b></div> <div style="text-align: right;"><b>93-03721</b> </div>					
14. SUBJECT TERMS Oxo Exchange/Linear Oxo Bridge/Fluxional/Transition Metal/ Xanthate Complex/Dithiocarbamate Complex				15. NUMBER OF PAGES 44	
				16. PRICE CODE --	
17. SECURITY CLASSIFICATION OF REPORT Unclassified	18. SECURITY CLASSIFICATION OF THIS PAGE Unclassified	19. SECURITY CLASSIFICATION OF ABSTRACT Unclassified	20. LIMITATION OF ABSTRACT --		

OFFICE OF NAVAL RESEARCH

Grant N00014-90-J-1762

R&T Code 4135025

TECHNICAL REPORT NO. 4

Intramolecular Bridge/Terminal Oxo Exchange within  
[MoV<sub>2</sub>O<sub>3</sub>]<sup>4+</sup> Complexes Containing Linear Oxo Bridges

by

Robert L. Thompson, Samkeun Lee, Steven J. Geib, and N. John Cooper

Submitted for publication in the Journal of American Chemical Society

Department of Chemistry  
University of Pittsburgh  
Pittsburgh, PA 15260

Reproduction in whole or in part is permitted for  
any purpose of the United States Government

This document has been approved for public release  
and sale; its distribution is unlimited

**Intramolecular Bridge/Terminal Oxo Exchange within  $[\text{MoV}_2\text{O}_3]^{4+}$   
Complexes Containing Linear Oxo Bridges**

Robert L. Thompson, Samkeun Lee, Steven J. Geib and N. John Cooper\*

Department of Chemistry  
University of Pittsburgh  
Pittsburgh, Pennsylvania 15260

Submitted to J. Am. Chem. Soc.

DTIC QUALITY INSPECTED 3

Accession For	
NTIS	<input checked="checked" type="checkbox"/>
ETIC	<input type="checkbox"/>
Univ.	<input type="checkbox"/>
Date	
Disc	
A-1	

## Abstract

Room temperature  $^{13}\text{C}$  NMR spectra of the  $d^1$ - $d^1$  dimer  $[\text{Mo}_2\text{O}_3\{\text{S}_2^{13}\text{CN}(\text{CH}_2\text{Ph})_2\}_4]$  (**1**) exhibit a broad singlet for the thiocarboxylate ligand. The molecule is fluxional, and in the low temperature limit this singlet is replaced by two asymmetrical doublets (with components at  $\delta$  207.4, 207.2 and 200.7, 199.7) assigned to the thiocarboxylate ligands with one S trans to the bridging oxo group and one S trans to the terminal oxo group respectively of the syn and the anti isomers of **1**. The barrier to exchange has been determined between 320 and 335 K from the width of the resonance in the fast exchange region, and the small entropic contribution to the barrier ( $\Delta H^\ddagger = 11.9 \pm 0.4 \text{ kcal mole}^{-1}$ ,  $\Delta S^\ddagger = -2.0 \pm 0.6 \text{ cal K}^{-1} \text{ mole}^{-1}$ ) argues strongly in favor of an intramolecular mechanism for the exchange reaction in which the thiocarbamate ligands are rendered equivalent by exchange of bridge and terminal oxo groups through a transition state in which the linear oxo bridge has been replaced by two bent oxo bridges. This interpretation is supported by the observation that the related xanthate complexes  $[\text{Mo}_2\text{O}_3(\text{S}_2^{13}\text{COEt})_4]$  (**4**) and  $[\text{Mo}_2\text{O}_3(\text{S}_2^{13}\text{CO}^i\text{Pr})_4]$  (**5**) participate in similar exchange processes with  $\Delta H^\ddagger = 11.1 \pm 0.3$  and  $12.9 \pm 0.4 \text{ kcal mole}^{-1}$  and  $\Delta S^\ddagger = -3.9 \pm 1.2$  and  $1.9 \pm 0.6 \text{ cal K}^{-1} \text{ mole}^{-1}$  respectively. The small entropic contribution is again consistent with an intramolecular mechanism, and the similarity in enthalpic parameters for **1**, **4** and **5** argues against a mechanism involving dissociation of the  $[\text{Mo}^{\text{V}}_2\text{O}_3]^{4+}$  dimers into  $[\text{Mo}^{\text{VI}}\text{O}_2]^{2+}$  and  $[\text{Mo}^{\text{IV}}\text{O}]^{2+}$  containing monomers since such disproportionations are ligand sensitive. Single crystal diffraction studies have been established that **1** (monoclinic space group  $P2_1/n$ ;  $a = 11.604$  (4) Å;  $b = 21.81$  (2) Å;  $c = 13.85$  (1) Å;  $\beta = 99.90$  (2) deg;  $Z = 2$ ;  $R = 4.37\%$ ) and **5** (monoclinic space group  $C2/c$ ;  $a = 25.508$  (5);  $b = 9.659$  (2);  $c = 14.986$  (4);  $\beta = 101.96$  (2) deg;  $Z = 4$ ;  $R = 5.52\%$ ) have anti and syn orientations respectively for the terminal oxo groups in the solid state. All three complexes exist as a mixture of syn and anti isomers in solution, establishing that there is only a small free energy difference between these geometries.

## Introduction

Oxo complexes play a central role in the biological and inorganic chemistry of molybdenum.<sup>1,2</sup> In the +5 oxidation state molybdenum oxo chemistry is dominated by the  $[\text{Mo}^{\text{V}}_2\text{O}_3]^{4+}$  unit, which contains a linear oxo bridge which spin pairs two  $d^1$  centers while two terminal oxo ligands adopt syn or anti orientations perpendicular to the oxo bridge.<sup>2-8</sup>

Our interest in  $[\text{Mo}^{\text{V}}_2\text{O}_3]^{4+}$  complexes, stimulated by the unusual photochromism we have observed for some examples<sup>9</sup> and by the potential utility of such properties in optical memory systems and other opto-electronic applications,<sup>10</sup> recently led us to examine the solution structures of  $[\text{Mo}^{\text{V}}_2\text{O}_3]^{4+}$  complexes by  $^{13}\text{C}$  NMR. We now wish to report that  $[\text{Mo}^{\text{V}}_2\text{O}_3]^{4+}$  complexes with both dithiocarbamate and xanthate ligands exhibit low energy intramolecular dynamic behavior, which we propose involves bridge for terminal oxo exchange, and that there is only a small free energy difference between the syn and anti isomers in the complexes examined.

## Experimental Section

**General Procedures.** All manipulations were carried out under a dry, oxygen-free nitrogen atmosphere by means of a Vacuum Atmosphere Drybox or standard Schlenk techniques. Toluene and hexane were distilled from potassium metal, and methylene chloride was distilled from  $\text{CaH}_2$  before use. Pentane was stirred over 5%  $\text{HNO}_3/\text{H}_2\text{SO}_4$ , then neutralized with  $\text{K}_2\text{CO}_3$  and distilled from  $\text{CaH}_2$  before use. Deuterated methylene chloride (99.9% D, MSD Isotopes) and chloroform (99.8% D, MSD Isotopes) were degassed by dry nitrogen purge and passed through basic activity I alumina to remove HCl before use. Labelled potassium dibenzylidithiocarbamate was prepared from  $^{13}\text{CS}_2$  (99.9%  $^{13}\text{C}$ , MSD Isotopes) and  $\text{HN}(\text{CH}_2\text{Ph})_2$  according to an adaptation of the procedure described by Colton and Scollary<sup>11</sup> and unlabelled potassium dibenzylidithiocarbamate was prepared similarly from  $\text{CS}_2$ .<sup>11</sup> Labelled potassium isopropylxanthate and ethylxanthate were prepared from  $^{13}\text{CS}_2$  and  $i\text{PrOH}$  according to an adaptation of the procedure described by Newton et al.<sup>12</sup> Microanalyses were performed by Atlantic Microlabs, Inc., Norcross, GA.

**Preparation of  $[\text{Mo}_2\text{O}_3\{\text{S}_2^{13}\text{CN}(\text{CH}_2\text{Ph})_2\}_4]\cdot\text{CH}_2\text{Cl}_2$  ( $1\cdot\text{CH}_2\text{Cl}_2$ ).**

Labelled  $\text{K}[\text{S}_2^{13}\text{CN}(\text{CH}_2\text{Ph})_2]$  was used to prepare  $[\text{Mo}_2\text{O}_3\{\text{S}_2^{13}\text{CN}(\text{CH}_2\text{Ph})_2\}_4]$  from  $\text{MoCl}_5$  in  $\text{H}_2\text{O}$  according to the procedure by Newton et al.<sup>12</sup> Samples of  $[\text{Mo}_2\text{O}_3\{\text{S}_2^{13}\text{CN}(\text{CH}_2\text{Ph})_2\}_4]$  were purified by recrystallization from a 3:1 mixture of pentane and  $\text{CH}_2\text{Cl}_2$  at  $-30^\circ\text{C}$ .  $^1\text{H}$  NMR ( $\text{CD}_2\text{Cl}_2$ , 300 MHz):  $\delta$  7.36 - 7.27 (m, 40 H, 8  $\text{C}_6\text{H}_5$ ), 4.97 (br m, 16 H, 8  $\text{CH}_2$ ).  $^{13}\text{C}\{^1\text{H}\}$  NMR ( $\text{CDCl}_3$ , 125 MHz):  $\delta$  226.8 (br s,  $\text{CS}_2$ ), 134.4 (s,  $\text{C}_6\text{H}_5$ ), 129.0 (s,  $\text{C}_6\text{H}_5$ ), 128.4 (s,  $\text{C}_6\text{H}_5$ ), 52.6 (s,  $\text{CH}_2$ ). Anal. Calcd for  $\text{C}_{60}\text{H}_{56}\text{Mo}_2\text{N}_4\text{O}_3\text{S}_8\cdot\text{CH}_2\text{Cl}_2$ : C, 51.80; H, 4.03; N, 3.96. Found: C, 52.10; H, 4.17; N, 4.00.

**Preparation of  $[\text{Mo}_2\text{O}_3\{\text{S}_2\text{CN}(\text{CH}_2\text{Ph})_2\}_4]\cdot\text{CH}_2\text{ClCH}_2\text{Cl}$**

( $1\cdot\text{CH}_2\text{ClCH}_2\text{Cl}$ ). Samples of unlabelled **1** for X-ray diffraction studies were prepared from  $\text{MoCl}_5$  in a manner identical to that described above for the  $^{13}\text{C}$  labelled metal, and crystals suitable for X-ray diffraction were grown by diffusion of hexane vapor into a saturated solution of **1** in  $\text{CH}_2\text{ClCH}_2\text{Cl}$ .

**Preparation of  $[\text{MoO}\{\text{S}_2\text{CN}(\text{CH}_2\text{Ph})_2\}_2]$  (**2**).** This compound was prepared by  $\text{PPh}_2\text{Et}$  reduction of  $[\text{MoO}_2\{\text{S}_2\text{CN}(\text{CH}_2\text{Ph})_2\}_2]$  in refluxing 1,2-dichloroethane by means of an adaptation of the procedure described by Chen et al. for  $[\text{MoO}(\text{S}_2\text{CNEt}_2)_2]$ .<sup>14</sup>  $^{13}\text{C}\{^1\text{H}\}$  NMR ( $\text{CDCl}_3$ , 75 MHz):  $\delta$  223.5 (br s,  $\text{CS}_2$ ), 133.6, 129.2, 128.7, 128.4 (all s,  $\text{C}_6\text{H}_5$ ), 52.8 (s,  $\text{CH}_2$ ).

**Preparation of  $[\text{MoO}_2\{\text{S}_2\text{CN}(\text{CH}_2\text{Ph})_2\}_2]$  (**3**).**  $\text{K}[\text{S}_2\text{C}(\text{CH}_2\text{Ph})_2]$  was used to prepare  $[\text{MoO}_2\{\text{S}_2\text{CN}(\text{CH}_2\text{Ph})_2\}_2]$  from  $\text{Na}_2\text{MoO}_4\cdot 2\text{H}_2\text{O}$  according to an adaptation of the procedure described by Moore and Larson.<sup>15</sup>  $^{13}\text{C}\{^1\text{H}\}$  NMR ( $\text{CD}_2\text{Cl}_2$ , 74.5 MHz):  $\delta$

199.9 (br s, CS<sub>2</sub>), 133.6 (s, C<sub>6</sub>H<sub>5</sub>), 129.3 (s, C<sub>6</sub>H<sub>5</sub>), 128.7 (s, C<sub>6</sub>H<sub>5</sub>), 128.4 (s, C<sub>6</sub>H<sub>5</sub>), 53.7 (s, CH<sub>2</sub>).

**Preparation of [Mo<sub>2</sub>O<sub>3</sub>(S<sub>2</sub><sup>13</sup>COEt)<sub>4</sub>] (4).** Labelled K[S<sub>2</sub><sup>13</sup>COEt] was used to prepare [Mo<sub>2</sub>O<sub>3</sub>(S<sub>2</sub><sup>13</sup>COEt)<sub>4</sub>] from Na<sub>2</sub>MoO<sub>4</sub>·2H<sub>2</sub>O according to an adaptation of the literature procedures.<sup>12,15</sup> Samples of [Mo<sub>2</sub>O<sub>3</sub>(S<sub>2</sub><sup>13</sup>COEt)<sub>4</sub>] were purified by recrystallization from a 2:1 mixture of pentane and toluene at -30°C. <sup>1</sup>H NMR (CD<sub>2</sub>Cl<sub>2</sub>, 300 MHz): δ 4.65 (br m, 8 H, 4 CH<sub>2</sub>), 1.49 (t, J = 7.1 Hz, 12 H, 4 CH<sub>3</sub>). <sup>13</sup>C{<sup>1</sup>H} NMR (CD<sub>2</sub>Cl<sub>2</sub>, 74.5 MHz): δ 227.1 (br s, CS<sub>2</sub>), 71.4 (s, CH<sub>2</sub>), 14.0 (s, CH<sub>3</sub>). Anal. Calcd for C<sub>12</sub>H<sub>20</sub>Mo<sub>2</sub>O<sub>7</sub>S<sub>8</sub>: C, 19.89; H, 2.79. Found: C, 19.91; H, 2.73.

**Preparation of [Mo<sub>2</sub>O<sub>3</sub>(S<sub>2</sub><sup>13</sup>CO<sup>*i*</sup>Pr)<sub>4</sub>]·C<sub>6</sub>H<sub>5</sub>CH<sub>3</sub> (5·C<sub>6</sub>H<sub>5</sub>CH<sub>3</sub>).** Labelled K[S<sub>2</sub><sup>13</sup>CO<sup>*i*</sup>Pr] was used to prepare [Mo<sub>2</sub>O<sub>3</sub>(S<sub>2</sub><sup>13</sup>CO<sup>*i*</sup>Pr)<sub>4</sub>] from Na<sub>2</sub>MoO<sub>4</sub>·2H<sub>2</sub>O according to an adaptation of the literature procedure.<sup>12,15</sup> Samples of [Mo<sub>2</sub>O<sub>3</sub>(S<sub>2</sub><sup>13</sup>CO<sup>*i*</sup>Pr)<sub>4</sub>] were purified by recrystallization from a 2:1 mixture of pentane and toluene at -30°C as a mono-toluene solvate. Diffraction quality crystals of unlabelled [Mo<sub>2</sub>O<sub>3</sub>(S<sub>2</sub>CO<sup>*i*</sup>Pr)<sub>4</sub>]·C<sub>6</sub>H<sub>5</sub>CH<sub>3</sub> (prepared similarly) were grown by the diffusion of hexane vapor into a saturated toluene solution of the complex within a sealed vessel at room temperature over a period of 10 days. Purple hexagonal prisms of [Mo<sub>2</sub>O<sub>3</sub>(S<sub>2</sub>CO<sup>*i*</sup>Pr)<sub>4</sub>]·C<sub>6</sub>H<sub>5</sub>CH<sub>3</sub> with a green lustre were collected by decantation, washed with pentane, and dried under vacuum. <sup>1</sup>H NMR (CD<sub>2</sub>Cl<sub>2</sub>, 300 MHz): δ 7.25 - 7.10 (m, 5 H, C<sub>6</sub>H<sub>5</sub>CH<sub>3</sub>), 5.51 (septet, J = 6.2 Hz, 4 H, CH), 2.34 (s, 3 H, CH<sub>3</sub>C<sub>6</sub>H<sub>5</sub>), 1.46 (d, J = 6.2 Hz, 24 H, 8 CH<sub>3</sub>, ). <sup>13</sup>C{<sup>1</sup>H} NMR (CDCl<sub>3</sub>, 74.5 MHz): δ 225.7 (br s, CS<sub>2</sub>), 79.8 (s, CH), 21.6 (s, CH<sub>3</sub>). Anal. Calcd for C<sub>23</sub>H<sub>36</sub>Mo<sub>2</sub>O<sub>7</sub>S<sub>8</sub>: C, 31.65; H, 4.16. Found: C, 31.22; H, 4.08.

**Variable Temperature NMR Studies.** <sup>1</sup>H spectra were recorded on a Bruker AF 300 spectrometer at 300 MHz. <sup>13</sup>C NMR spectra were recorded on a Bruker AF300 or 500

spectrometer at 74.5 or 125 MHz respectively. Temperatures within the NMR probe were controlled by a Bruker variable temperature unit, which was calibrated against boiling and freezing distilled H<sub>2</sub>O and is accurate to within 0.2°C. Samples were allowed to equilibrate thermally at each temperature for 10 minutes before spectra were recorded. The high temperature range was limited to 325 K in CDCl<sub>3</sub>, 305 K in CD<sub>2</sub>Cl<sub>2</sub>, and 335 K in 1,2-dichloroethane by the solvent boiling points. Low temperature spectra were recorded down to 210 K in CD<sub>2</sub>Cl<sub>2</sub>, 225 K in CDCl<sub>3</sub>, below which further changes became negligible. Exchange barriers were calculated from the linewidths of <sup>13</sup>C resonances arising from exchanging sites using the appropriate equations as follows.

In the case of exchange processes with equal populations in both sites, as established by integration of the low temperature spectrum, the linewidth at the lower limit was assumed to be the linewidth in the absence of exchange,  $w_{1/2}^0$ , and was used to calculate  $T_2^{\text{eff}}$ .<sup>16,17</sup>

$$T_2^{\text{eff.}} = 1/(\pi w_{1/2}^0)$$

This value was then used to calculate the rate of exchange,  $k$ , below coalescence using the slow exchange limit approximation.<sup>16,17</sup>

$$k = \pi w_{1/2} - 1/T_2^{\text{eff.}}$$

The rate of exchange above coalescence was calculated according to the fast exchange approximation<sup>16,17</sup> using the value of  $w_{1/2}^0$  obtained above coalescence and the value of  $\Delta\nu$  obtained in the low temperature limit.

$$k = \pi(\Delta\nu)^2 / 2(w_{1/2} - w_{1/2}^0)$$

For comparison with the linewidth data the rate of exchange at coalescence was also calculated using the frequency difference between the resonances below coalescence,  $\Delta\nu$ , and assuming equal forward and reverse exchange rates so that:<sup>16,17</sup>

$$k = \pi\Delta\nu/2^{1/2} = 2.22\Delta\nu$$



The free energies of activation ( $\Delta G^\ddagger$ ) for the exchange processes at each temperature were calculated from exchange rates by means of the Eyring equation,<sup>18</sup> taking the transmission coefficient  $\kappa = 1$  as is usual in dynamic NMR studies.<sup>16</sup> The activation enthalpies and entropies ( $\Delta H^\ddagger$  and  $\Delta S^\ddagger$ ) were calculated from the intercept and slope of plots of  $\Delta G^\ddagger$  vs. temperature, treating the values above and below coalescence as separate data sets. The uncertainties in  $\Delta G^\ddagger$  were calculated as outlined in reference 17, equation 111.

In the case of exchange processes with unequal populations in exchanging sites (as indicated by unequal peak integrations) the temperatures at which spectra with measurable linewidths for the smaller peaks could be recorded were few, and free energies of activation were approximated by means of the method described by Shanan-Atidi and Bar-Eli.<sup>19</sup> These free energies of activation for disappearance of the two different species in the secondary exchanges were estimated as follows:

$$\Delta G^\ddagger_A = 4.57T_c \{ 10.62 + \log[\Delta\nu/k_A(1-\Delta P)] + \log(T_c/\Delta\nu) \}$$

$$\Delta G^\ddagger_B = 4.57T_c \{ 10.62 + \log[\Delta\nu/k_B(1+\Delta P)] + \log(T_c/\Delta\nu) \}$$

where  $T_c$  is the coalescence temperature,  $k_A$  and  $k_B$  are the rate constants obtained using the slow exchange limit approximation for the signals A and B,<sup>16,17</sup> and  $\Delta P$  is the population difference calculated from the relative integrated areas of signals A and B. The uncertainties for these  $\Delta G^\ddagger$  values are estimated to be ca 20%.

**X-Ray Diffraction Studies.** Deep purple crystals with a green luster of  $C_{60}H_{56}Mo_2N_4O_3S_8 \cdot CH_2ClCH_2Cl$  ( $1 \cdot CH_2ClCH_2Cl$ ) and  $C_{16}H_{28}Mo_2O_7S_8 \cdot C_6H_5CH_3$  ( $5 \cdot C_6H_5CH_3$ ) were coated in epoxy cement and attached to fine glass fibers. Diffraction data were collected for each crystal as summarized in Table I.

$\text{I} \cdot \text{CH}_2\text{ClCH}_2\text{Cl}$  was uniquely assignable to monoclinic group  $\text{P}2_1/\text{a}$  on the basis of systematic absences. On the basis of systematic absences and of photographic evidence **5** was assignable to the monoclinic space group  $\text{C}2/\text{c}$  or  $\text{Cc}$ . Centrosymmetric  $\text{C}2/\text{c}$  was chosen on the basis of  $E$ -values and the successful solution and refinement of the structure. Unit cell dimensions were derived from the least squares fit of the angular settings of 25 reflections with  $18^\circ \leq 2\theta \leq 25^\circ$  for both crystals. A profile fitting procedure was applied to all data to improve the precision of the measurement of weak reflections. A semi-empirical absorption correlation (XEMP) was applied to the diffraction data. Diffraction data were corrected for extinction effects.

Both structures were studied by means of the direct methods routine TREF which located the Mo atoms. The remaining non-hydrogen atoms were located from subsequent Fourier syntheses and refined isotropically. Hydrogen atoms were placed in idealized calculated positions ( $d(\text{C-H}) = 0.96\text{\AA}$ ). The final difference Fourier syntheses for both compounds showed only diffuse backgrounds. Inspections of  $E_o$  vs  $E_c$  values and trends based on  $\sin \theta$ , Miller indices and parity groups failed to reveal any systematic errors in the X-ray data for either crystal. Atomic coordinates are listed in Tables II and V, selected bond lengths in Tables III and VI, and selected bond angles in Tables IV and VII. All computer programs used in the collection, solution and refinement of crystal data are contained in the Siemens program packages SHELXTL PLUS (VMS version 4.2).

## Results and Discussion

An early theoretical study of a structurally characterized example suggested that the dihedral angle between the two  $\text{O}_t\text{MoO}_b$  ( $\text{O}_t$  = terminal oxo,  $\text{O}_b$  = bridging oxo) planes in  $[\text{Mo}^{\text{V}}_2\text{O}_3]^{4+}$  complexes must be close to  $0^\circ$  or  $180^\circ$  if the single valence electron at each metal center is to be spin paired,<sup>4</sup> and X-ray diffraction studies have indeed established that subsequently characterized examples of these complexes adopt either syn or anti geometries in the solid state.<sup>15-21</sup> The local coordination sphere around the Mo atoms within the

$[\text{M}_2\text{O}_3]^{4+}$  core approximates an octahedron, with the remaining coordination sites most typically filled by the sulfur atoms of a bis-chelate dithio ligand such as a dithiophosphate, an xanthate, or a dithiocarbamate as shown by the selected examples in Scheme 1<sup>4,5,7</sup> (although many examples have demonstrated that  $[\text{MoV}_2\text{O}_3]^{4+}$  complexes are not limited to such ligand systems<sup>8</sup> and recent examples can be found, for example, in Schiff base systems<sup>2</sup>).

There is a clear distinction in both the syn and the anti geometries between bis-chelate ligand molecules which have one sulfur atom trans to the bridging oxo and those which have one sulfur trans to a terminal oxo. We were accordingly surprised to discover, in the course of studies of photodisproportionation of the dithiocarbamate complex  $[\text{Mo}_2\text{O}_3\{\text{S}_2\text{CN}(\text{CH}_2\text{Ph})_2\}_4]$  (**1**)<sup>9</sup>, that <sup>1</sup>H NMR spectra of **1** exhibited a single rather broad absorption for the benzylic hydrogens of the dithiocarbamate ligands and similarly undifferentiated absorptions for the phenyl groups. This led us to speculate that the complexes were undergoing a previously unreported fluxional process, and hence to a <sup>13</sup>C NMR study of the solution structure of **1**. Carbon NMR was the spectroscopy of choice because of the simplicity anticipated for spectra in the low temperature limit, but the limited solubility of **1** (even in moderately polar solvents such as  $\text{CH}_2\text{Cl}_2$ ) and the low sensitivity of natural abundance <sup>13</sup>C NMR required the use of samples which had been enriched at the dithiocarboxy positions by preparation of the ligand from 99.9 atom % <sup>13</sup>CS<sub>2</sub>.

**Variable Temperature <sup>13</sup>C NMR Spectra of  $[\text{Mo}_2\text{O}_3\{\text{S}_2^{13}\text{CN}(\text{CH}_2\text{Ph})_2\}_4]$  and Evidence for Bridge/Terminal Oxo Exchange and Syn/Anti Isomerization.**

Room temperature <sup>13</sup>C NMR spectra of **1** exhibited a single, broad absorption at  $\delta$  203.8 assignable to the enriched carbon of the dithiocarbamate ligand. As the temperature is lowered (Figure 1), the broad singlet collapses and two new resonances of equal intensity appear at  $\delta$  207.4 and  $\delta$  199.8 at 250 K. As the temperature is lowered further, these signals separate again into two pairs of resonances which this time are of unequal intensity

with the stronger signals at  $\delta$  207.4 and 199.7 and the weaker signals at  $\delta$  207.2 and  $\delta$  200.7, respectively at 220 K. The magnitude of this secondary splitting is slight. All the temperature dependent behavior is fully reversible upon warming.

The initial splitting of the room temperature singlet into two equal intensity resonances suggested that the molecule is stereochemically non-rigid and undergoes an inter or intramolecular dynamic process which equilibrates the dithiocarbamate ligands which have sulfur trans to the bridging oxo with the dithiocarbamate ligands with sulfur trans to the terminal oxo. Assignment of the quaternary signals at  $\delta$  207.4 and  $\delta$  199.8 to the dithiocarbamate ligands with a sulfur trans to the bridging oxo and to the dithiocarbamate ligands with a sulfur trans to the terminal oxo respectively is based on comparison with the quaternary  $^{13}\text{C}$  NMR resonances for the Mo(IV) and Mo(VI) complexes  $[\text{MoO}(\text{S}_2\text{CN}(\text{CH}_2\text{Ph})_2)_2]$  (2) and  $[\text{MoO}_2(\text{S}_2\text{CN}(\text{CH}_2\text{Ph})_2)_2]$  (3) at  $\delta$  223.5 and  $\delta$  201.8 - the average room temperature resonance for the Mo(V) complex **1** at  $\delta$  203.8 is in between these resonances and it seems probable that the dithiocarbamate with a sulfur trans to the terminal oxo group is in the chemical environment which most closely resembles that in the Mo(VI) complex and hence has the higher field resonance.

The secondary splitting of the dithiocarbamate ligands into unequally populated groups was initially puzzling, but simple theory,<sup>4</sup> as mentioned above, does not require a significant energy difference between the syn and anti conformations of the  $[\text{Mo}^{\text{V}}_2\text{O}_3]^{4+}$  core and a reasonable interpretation is that **1** exists in solution as a mixture of the syn and anti isomers, and that these are equilibrated above the coalescence point by the same dynamic process responsible for exchange of the dithiocarbamate ligands or by a second dynamic process (see below).

**Possible Inter and Intramolecular Bridge/Terminal Oxo Bridge Mechanisms within  $[\text{Mo}_2\text{O}_3(\text{S}_2\text{CN}(\text{CH}_2\text{Ph})_2)_2]$ .** The two most obvious candidates for the primary exchange process are shown in Scheme II and Scheme III

respectively. The first is an intermolecular process which involves the known ability of  $[\text{Mo}^{\text{V}}_2\text{O}_3]^{4+}$  complexes to participate in thermal disproportionation equilibria which give  $[\text{Mo}^{\text{VI}}\text{O}_2]^{2+}$  and  $[\text{Mo}^{\text{IV}}\text{O}]^{2+}$  complexes,<sup>20-22</sup> and the second is an intramolecular pathway in which the dimer bends until one terminal oxo group coordinates to the other Mo center to give a dinuclear intermediate or transition state containing a six-coordinate Mo(IV) center and a seven-coordinate Mo(VI) center<sup>23</sup> connected by two bridging oxo atoms. Such an intermediate or transition state is highly plausible, given that examples of Mo(V) oxo dimers with four oxo groups rather than three (i.e.  $[\text{Mo}_2\text{O}_4]^{2+}$  rather than  $[\text{Mo}_2\text{O}_3]^{4+}$  cores) characteristically have two bridging oxo atoms as established crystallographically for a number of examples.<sup>8g,25</sup> This intermediate places both ligands at the six-coordinate Mo(IV) center trans to a bridging oxo atom. If the process is now reversed (with dissociation of the oxo atom that had originally been bridging) bridge and terminal oxo groups on one Mo atom will have exchanged and the corresponding dithiocarbamate ligands will also have exchanged.

**Distinguishing Between Intermolecular and Intramolecular Exchange Mechanisms within  $[\text{Mo}_2\text{O}_3\{\text{S}_2^{13}\text{CN}(\text{CH}_2\text{Ph})_2\}_4]$ .** Although the key dissociative step in Scheme II is well precedented, it seemed unlikely that a dissociative process could provide a kinetically competent pathway for the dynamic process. The dissociation constants for the closely related Mo(V) dimers  $[\text{Mo}_2\text{O}_3(\text{S}_2\text{CNPr}_2)_4]$ <sup>20</sup> and  $[\text{Mo}_2\text{O}_3(\text{S}_2\text{CNEt}_2)_4]$ <sup>21</sup> have been established to be  $4.8 \times 10^{-3}$  mole  $\text{L}^{-1}$  in chlorobenzene and  $2.0 \times 10^{-3}$  mole  $\text{L}^{-1}$  in 1,2-dichloroethane respectively. It therefore seemed unlikely that there would be a sufficient concentration of the disproportionation products **2** and **3** to allow rapid dissociative isomerization of **1** - we do see some **3** in  $^{13}\text{C}$  NMR spectra of labelled **1** (e.g. at  $\delta$  199.8 in Figure 1), but this **3** is a byproduct of decomposition of **1** in halocarbon NMR solvents, as established by its slow increase over time. We see no **2** as would be anticipated if the disproportionation equilibrium were readily accessible thermally.

Direct experimental support for an intramolecular isomerization pathway within **1**, such as that in Scheme III, comes from the value of the exchange barrier as determined from the linewidth of the resonance of the averaged quaternary carbons above coalescence and of the quaternary carbons trans to the terminal or bridging oxo groups below coalescence. Data suitable for qualitative analysis were obtained in  $\text{CH}_2\text{ClCH}_2\text{Cl}$  and are summarized in Table VIII, together with the derived exchange rates and  $\Delta G^\ddagger$  obtained as described in the Experimental Section (linewidths determined in  $\text{CD}_2\text{Cl}_2$  gave values for  $\Delta G^\ddagger$  indistinguishable from those in  $\text{CH}_2\text{ClCH}_2\text{Cl}$  but were only available over a restricted range of temperatures in this low boiling solvent). The small magnitude ( $12.2 \text{ kcal mole}^{-1}$  above coalescence) of  $\Delta G^\ddagger$  for the exchange constitutes an immediate argument against the intermolecular mechanism in Scheme II - Matsuda et al.<sup>21,22</sup> have previously reported a value of  $17.0 \pm 2.1 \text{ kcal mole}^{-1}$  for  $\Delta G^\ddagger$  for disproportionation of the closely related complex  $[\text{Mo}_2\text{O}_3(\text{S}_2\text{CNEt}_2)_4]$  in 1,2-dichloroethane at  $25^\circ\text{C}$ , and the comparison between this value and the data in Table VIII confirms our opinion that disproportionation does not provide a kinetically competent initial step for the exchange process in **1**.

The agreement between the activation barriers in Table VIII determined from linewidths above and below coalescence are acceptable but not outstanding, and this probably reflects systematic errors in values determined using the slow exchange approximation. These arise because of the influence on linewidths of the incipient splitting of the  $\delta$  207.4 and  $\delta$  199.8 peaks into components arising from the syn and anti isomers. We therefore prefer the values determined in the fast exchange approximation.

The availability of  $\Delta G^\ddagger$  values at several temperatures within the range covered by the fast exchange approximation in 1,2-dichloroethane allowed separation of  $\Delta G^\ddagger$  into its enthalpic and entropic components (Table IX) and hence provided further support for an intramolecular exchange mechanism. As is obvious from the insensitivity of  $\Delta G^\ddagger$  to variations in temperature  $\Delta S^\ddagger$  is negligible - this argues strongly against an intermolecular mechanism for the exchange process.

**The Relationship Between Syn/Anti Isomerization and Bridge/Terminal Oxo Exchange within  $[\text{Mo}_2\text{O}_3\{\text{S}_2^{13}\text{CN}(\text{CH}_2\text{Ph})_2\}_4]$ .** The intramolecular bridge/terminal oxo exchange reaction in Scheme III allows simultaneous syn/anti isomerization, a reaction which must be rapid on the NMR time scale if we are to average the signals from these isomers as the temperature of the sample is raised above that at which the low temperature limiting spectrum is observed.

The proposal that the observed syn/anti isomerization is a by-product of bridge/terminal oxo exchange was attractive because of its simplicity, but it seemed plausible initially that syn/anti isomerization could involve a second dynamic process such as counter-rotation of the two Mo coordination spheres about the Mo-O-Mo axis. We have, however, determined (as described in the Experimental Section) that the secondary exchange barrier is  $15.8 \pm 3$  kcal mole<sup>-1</sup>, a value close to that determined for the primary exchange process. The equality of these primary and secondary barriers establishes that it is unnecessary to hypothesize syn/anti isomerization mechanisms beyond that shown in Scheme III, although it remains possible (if unlikely) that rotation is a kinetically accessible syn/anti isomerization mechanism under these conditions and happens to have activation parameters similar to those for bridge/terminal oxo exchange.

**Ground State Isomers of  $[\text{Mo}_2\text{O}_3\{\text{S}_2\text{CN}(\text{CH}_2\text{Ph})_2\}_4]$  in the Solid State and in Solution.** The observation of facile interconversion of syn and anti isomers of **1** in solution led us to determine the molecular structure of **1** in the solid state by means of the single crystal X-ray diffraction study described in the Experimental Section. This enabled us to determine that **1** has the molecular structure shown in Figure 2 and that the crystal contains a molecule of 1,2-dichloroethane of solvation per dimer unit. Complex **1** resides on a crystallographic inversion center at (0, 1, 1/2). This requires that the Mo(1)-O(1)-Mo(2) angle be exactly 180°. Each Mo atom has a distorted octahedral coordination

geometry with cis angles ranging from 67.2 (1) to 110.7 (2)° and trans angles ranging from 155.0 (1) to 157.9 (2)°. The terminal Mo=O<sub>t</sub> bond length of 1.677 (5) Å agrees well with other Mo=O<sub>t</sub> bond lengths in the literature, and the Mo-O<sub>b</sub> bond length of 1.863 (2) Å is within the range reported for analogous distances in other [Mo<sup>V</sup><sub>2</sub>O<sub>3</sub>]<sup>4+</sup> complexes.<sup>3-8</sup> The Mo-S(2) bond, trans to M=O<sub>t</sub> (2), is 2.710 (3) Å, while the remaining Mo-S bonds range from 2.444 (3) to 2.506 (3) Å.

The most interesting feature of the molecular structure of **1** is the anti orientation adopted by the Mo=O<sub>t</sub> groups. This is analogous to the anti orientation which we have previously established for the [W<sub>2</sub>O<sub>3</sub>]<sup>4+</sup> groups in [W<sub>2</sub>O<sub>3</sub>{S<sub>2</sub>CN(CH<sub>2</sub>Ph)<sub>2</sub>}]<sub>4</sub>,<sup>9</sup> isologous with **1**, and to the anti orientations established for dithiophosphate and thiocyanate dimers,<sup>5,6</sup> but is in sharp contrast with the syn orientation adopted by other structurally characterized dithiocarbamate complexes of the [Mo<sup>V</sup><sub>2</sub>O<sub>3</sub>]<sup>4+</sup> unit.<sup>7</sup>

This is an intriguing observation, and the fact that the preference for an anti conformation is independent of the metal in **1** and its W isolog but that dithiocarbamate complexes of [Mo<sub>2</sub>O<sub>3</sub>]<sup>4+</sup> units with other R groups adopt a syn conformation<sup>7</sup> is consistent with the earlier assumption<sup>4</sup> that syn/anti preferences in [M<sub>2</sub>O<sub>3</sub>]<sup>4+</sup> complexes are not controlled by electronic factors. The solid state preferences must arise from combinations of secondary effects such as intramolecular steric interactions and solid state packing forces, and the syn/anti mixture observed in solutions of **1** at -28°C establishes that the free energy differences between the isomers in solution at this temperature is only 0.6 kcal mole<sup>-1</sup>. This small ΔG makes it meaningless to infer the identity of the major isomer in solution on the basis of the solid state structure.

**Variable Temperature <sup>13</sup>C NMR Spectra of the Xanthate Complexes [Mo<sub>2</sub>O<sub>3</sub>(S<sub>2</sub><sup>13</sup>COEt)<sub>4</sub>] and [Mo<sub>2</sub>O<sub>3</sub>(S<sub>2</sub><sup>13</sup>CO<sup>*i*</sup>Pr)<sub>4</sub>].** The evidence in favor of an intramolecular mechanism for bridge/terminal oxo exchange within **1** raised the question of whether such exchange reactions are a general characteristic of the [Mo<sup>V</sup><sub>2</sub>O<sub>3</sub>]<sup>4+</sup> unit within



other ligand environments, and hence suggested carbon NMR studies of other  $[\text{Mo}_2\text{O}_3]^{4+}$  complexes.

Xanthate complexes are attractive candidates for such studies since the dithiocarboxylate ligands can be prepared with  $^{13}\text{C}$  labels by a simple addition of alkoxides to  $^{13}\text{CS}_2$ .<sup>12,15</sup> More significantly, xanthate ligands are sufficiently similar to dithiocarbamates that we could anticipate bridge/terminal oxo exchange reactions similar to those observed for **1** if the reaction is intramolecular, but Mo(VI) monomers of the type  $[\text{Mo}^{\text{VI}}\text{O}_2(\text{S}_2\text{COR})_4]$  are believed to be unstable (largely because of the failure of attempts to prepare them),<sup>14,15</sup> and xanthate complexes of  $[\text{Mo}^{\text{V}}_2\text{O}_3]^{4+}$  cores are therefore less likely to participate in disproportionation equilibria which would allow access to intermolecular bridge/terminal exchange mechanisms such as that shown in Scheme II.

The particular xanthate dimers chosen for study were the ethyl complex  $[\text{Mo}_2\text{O}_3(\text{S}_2^{13}\text{COEt})_4]$  (**4**), one of the most extensively studied xanthate complexes,<sup>4,15</sup> and the isopropyl complex  $[\text{Mo}_2\text{O}_3(\text{S}_2^{13}\text{CO}^i\text{Pr})_4]$  (**5**),<sup>17</sup> chosen because the increased bulk of the ligand might shed some light on the importance of intramolecular steric bulk in these systems.

The quaternary carbon of the ethyl xanthate complex **4** gives rise to a  $^{13}\text{C}$  signal in  $\text{CDCl}_3$  at  $\delta$  227.1 at 300 K. This signal sharpens upon warming, and splits into singlets of equal intensity at  $\delta$  231.2 and 220.7 as the temperature is lowered to 260 K (Figure 3). These signals split further into high intensity singlets at  $\delta$  231.3 and 220.3 and weaker singlets at  $\delta$  230.9 and 222.0 as the temperature is lowered further to 230 K. Similarly, the quaternary carbon of the isopropylxanthate complex **5** gives a  $^{13}\text{C}$  signal in  $\text{CDCl}_3$  at  $\delta$  225.7 at 290 K. This signal again sharpens upon warming and splits into singlets of equal intensity at  $\delta$  229.8 and  $\delta$  220.3 as the temperature is lowered (Figure 4), in this case to 250 K. The upfield signal is split further at lower temperatures into a large singlet at  $\delta$  219.4 and a small singlet at  $\delta$  221.0. The downfield singlet does not split further, but a shoulder appears on its upfield side.

The temperature dependent  $^{13}\text{C}$  NMR spectra of **4** and **5** indicate that both xanthate complexes are fluxional and that xanthate ligands trans to bridging oxo groups exchange rapidly on the NMR trans scale with xanthate groups trans to terminal oxo groups. Since Mo(VI) xanthate oxo compounds are unknown we do not have a reference set of Mo(VI)  $^{13}\text{C}$  data with which to make comparisons, but we again assign the higher field resonances to ligands trans to terminal oxo groups by analogy with the dithiocarbamate data above.

The secondary splittings of the xanthate resonances into sets of peaks of unequal intensity again suggest that the complexes exist as an equilibrium mixture of syn and anti isomers in solution.

**Ground State Isomers of  $[\text{Mo}_2\text{O}_3(\text{S}_2\text{O}^i\text{Pr})_4]$  in the Solid State and in Solution.** It has been previously established that the ethyl xanthate complex **4** adopts a syn conformation in the solid state,<sup>4</sup> but the increased bulk of the isopropyl ligand in **5** raised the possibility that **5** might adopt an anti conformation in the solid state. We therefore carried out the single crystal X-ray diffraction study described in the Experimental Section, and established that **5** adopts a similar syn conformation in the solid state (Figure 5). This indicates that the increase in the bulk of the alkyl substituent on going from the ethylxanthate complex **4** to the isopropyl xanthate complex **5** does not give rise to sufficient intramolecular steric intervention to disfavor the syn isomer in the solid state.

As in the case of **1** it is tempting to assume a relationship between the solid state syn conformational preferences of **4** and of **5** and their solution conformational preferences, but the observation of both conformers of **4** and of **5** in solution establishes that there is only a small intrinsic free energy difference between the two conformers with both ligands (0.9 and 1.0 kcal mole<sup>-1</sup> respectively for **4** and **5**) and hence that the solid state preference could be controlled by minimal differences in packing energies rather than by an intramolecular electronic or steric factors.

Details of the solid state structure of **5** are unexceptional. There is one-half of a molecule in the asymmetric unit with a crystallographic two-fold axis along  $1/2, y, 3/4$ . There is an essentially linear oxo bridge of  $171.6(5)^\circ$  between the Mo centers, and a torsion angle of  $8.3^\circ$  between the terminal oxo atoms as viewed along the Mo-O-Mo axis. The Mo atoms have distorted octahedral coordination geometries with Mo-O<sub>b</sub> bond lengths of 1.877 (1) Å and Mo-O<sub>t</sub> bond lengths of 1.684 (6) Å. These parameters reflect the partial double bond character of the bridging oxo bonds and the full double bond character of the terminal oxo bonds. The Mo-S bond lengths vary, with the Mo-S(4) bond trans to the Mo=O<sub>t</sub> bond much the longest at 2.728 (2) Å while the remaining Mo-S bonds range from 2.455 (2) to 2.540 (2) Å. There is a disordered solvent molecule, believed to be toluene, which was not refined.

**Kinetic Parameters for the Fluxional Processes within [Mo<sub>2</sub>O<sub>3</sub>(S<sub>2</sub><sup>13</sup>COEt)<sub>4</sub>] and [Mo<sub>2</sub>O<sub>3</sub>(S<sub>2</sub><sup>13</sup>CO<sup>*i*</sup>Pr)<sub>4</sub>].** The resemblance between the variable temperature <sup>13</sup>C NMR spectra of **4** and **5** and those of **1** is quantitative as well as qualitative. Exchange rates for the primary dynamic process equilibrating xanthate ligands with a sulfur trans to a terminal oxo with xanthates with a sulfur trans to a bridging oxo were determined at a variety of temperatures both from linewidth measurements and from coalescence temperatures as described in the Experimental Section, and these rates and the derived free energy barriers to exchange are summarized in Tables X and XI for complexes **4** and **5** respectively. Inspection of these tables establishes that the  $\Delta G^\ddagger$  are indistinguishable for **4** and **5**, and at *ca* 12.3 kcal mole<sup>-1</sup> above coalescence are essentially identical to the corresponding value of 12.6 kcal mole<sup>-1</sup> for **1**. We have also used the values of  $\Delta G^\ddagger$  determined from linewidth measurements above coalescence (which we prefer for reasons discussed above in the case of **1**) to determine the enthalpic and entropic contributions to  $\Delta G^\ddagger$  as summarized in Table IX.

The activation parameters for the dynamic processes occurring within **4** and **5** strongly suggest that these are intramolecular processes since there are only negligible entropic

contributions to the activation barriers, and we propose that they involve a bridge/terminal oxo exchange mechanism analogous to that outlined for **1** in Scheme III. This would account for both the xanthate exchange reaction and for the syn/anti isomerization which appears as a secondary process. The precision of the data do not allow a highly precise independent determination of the syn/anti exchange barriers in **4** and **5**, but we have been able to determine approximate values of  $\Delta G^\ddagger$  as described in the Experimental Section. The resulting free energies of activation (Table XII - this includes the data for **1** for comparison) are identical within experimental error to those determined for the primary exchange process, and the data do not require the hypothesis of a syn/anti isomerization mechanism beyond that provided by the intramolecular bridge/terminal oxo exchange reaction shown in Scheme III.

### Conclusion.

The dithiocarbamate and xanthate  $[\text{MoV}_2\text{O}_3]^{4+}$  complexes **1**, **4** and **5** are all fluxional on the NMR time scale, and participate in dynamic processes which equilibrate the bis-chelate ligands. For all three compounds the activation parameters associated with this dynamic process strongly suggest an intramolecular mechanism which we propose involves the bridge for terminal oxo exchange reaction shown in Scheme III. This would also result in interconversion of the syn and anti isomers of **1**, **4** and **5**, a process which is indeed observed to be fast on the NMR time scale for all three complexes.

The most convincing argument in favor of an intramolecular bridge/terminal oxo exchange process to account for the fluxionality of **1**, **4** and **5** is the marked similarity of the parameters determined for the dithiocarbamate complex **1** and for the xanthate complexes **4** and **5**. It is well established that the disproportionation equilibria of  $[\text{MoV}_2\text{O}_3]^{4+}$  complexes are highly sensitive to the ancillary ligands, and the similarity of the parameters would be a remarkable coincidence if the exchange process is dissociative (Scheme II) rather than intramolecular as shown in Scheme III.

Intramolecular bridge/terminal oxo exchange in  $[\text{Mo}^{\text{V}}_2\text{O}_3]^{4+}$  complexes has not previously been proven, and its existence, facility and probable generality adds an interesting dimension to the chemistry of this class of molecules. These systems are of considerable interest in their own right, and although they do not participate directly in the Mo(VI)/Mo(IV) oxo transfer reactions central to the chemistry of molybdenum based oxo transferases, understanding their chemistry is critical to our understanding of the biological systems because of the pervasive formation of  $[\text{Mo}^{\text{V}}_2\text{O}_3]^{4+}$  complexes by comproportionation of  $[\text{Mo}^{\text{VI}}\text{O}_2]^{2+}$  and  $[\text{Mo}^{\text{IV}}\text{O}]^{2+}$  monomers, as has been recently emphasized.<sup>2</sup>

**Acknowledgments.** This work was supported in part by the Office of Naval Research.

**Supplementary Material Available:** Complete Tables of bond lengths (Tables IS, IIS); complete Tables of bond angles (Tables IIIS, IVS) anisotropic displacement coefficients (Tables VS, VIS); hydrogen atom coordinates and isotropic thermal parameters (Tables VIIS, VIIIS); and observed and calculated structure factors (Table IXS, XS). Ordering information is given on any current masthead page.

## References and Notes

- (1) (a) Bray, R. C. in The Enzymes, 3rd Ed.; P.D., Ed.; Academic Press: New York, 1975; Vol. XII, Part B, Chap 6. (b) Stiefel, E. I. Prog. Inorg. Chem. **1977**, 22, 1. (c) Coughlan, M. P. Ed.; Molybdenum and Molybdenum Containing Enzymes; Pergamon Press: New York, 1980. (d) Newton, W. E.; Otsuka, S., Molybdenum Chemistry of Biological Significance; Plenum Press: New York, 1980. (e) Garner, C. D.; Charnock, J. M. In Comprehensive Coordination Chemistry Wilkinson, G.; Gillard, R. D.; McCleverty, J., Eds.; Pergamon: Oxford, 1987; Vol. 3, Part 36.4. (f) Holm, R. H. Coord. Chem. Rev. **1990**, 100, 183.
- (2) Craig, J. A.; Harlan, E. W.; Snyder, B. S.; Whitener, M. A.; Holm, R. H. Inorg. Chem. **1989**, 28, 2082.
- (3) Holm, R. H. Chem. Rev. **1987**, 87, 1401.
- (4) Blake, A. B.; Cotton, F. A.; Wood, J. S. J. Am. Chem. Soc. **1964**, 86, 3024.
- (5) (a) Knox, J. R.; Prout, C. K. Acta Crystallogr. B **1969**, B25, 2281. (b) Aliev, Z. G.; Atovmyan, L. O.; Tkachev, V. V. Zh. Strukt. Khim **1975**, 16, 694. (c) Thompson, R. L.; Geib, S.J.; Cooper, N. J. Chem. Mater., submitted.
- (6) Bino, A.; Cohen, S.; Tsimering, L. Inorg. Chim. Acta **1983**, 77, L79.
- (7) (a) Ricard, L.; Estienne, J.; Karagiannidis, P.; Toledano, P.; Fischer, J.; Mitschler, A.; Weiss, R. J. Coord. Chem. **1974**, 3, 227. (b) Garner, C. D.; Howlader, N. C.; Mabbs, F. E.; McPhail, A. T.; Onan, K. D. J. Chem. Soc. Dalton Trans. **1979**, 962.
- (8) Zubieta, J. A.; Maniloff, G. B. Inorg. Nucl. **1976**, 12, 121. (b) Cotton, F. A.; Fanwick, P. E.; Fitch, J. W., III Inorg. Chem. **1978**, 17, 3254. (c) Tsao, Y. Y.-P.; Fritchie, C. J., Jr.; Levy, H. A. J. Am. Chem. Soc. **1978**, 100, 4089. (d) Tatsumisago, M.; Matsubayashi, G.; Tanaka, T.; Nishigaki, S.; Nakatsu, K. J. Chem. Soc. Dalton Trans. **1982**, 121. (e) Dahlstron, P. L.; Hyde, J. R.; Vella, P. A.; Zubieta, J. Inorg. Chem. **1982**, 21, 927. (f) Kamenar, B.; Penavic, M.; Korpar-Colig, B.; Markovic, B. Inorg. Chim. Acta **1982**, 65, L245. (g) Lincoln, S.; Koch, S. A. Inorg.

- Chem. **1986**, 25, 1594. (h) Baird, D. M.; Rheingold, A. L.; Croll, S. D.; DiCeuso, A. T. Inorg. Chem. **1986**, 25, 3458. (i) El-Essawi, M. M.; Weller, F.; Stahl, K.; Kersting, M.; Dehnicke, K. Z. Anorg. Allg. Chem. **1986**, 542, 175. (j) Mattes, R.; Scholard, H.; Mikloweit, U.; Schrenk, V. Z. Naturforsch. **1987**, 42B, 599.
- (9) Lee, S. K.; Staley, D. L.; Rheingold, A. L.; Cooper, N. J. Inorg. Chem. **1990**, 29, 4391.
- (10) (a) Photochromism-Molecules and Systems; Dürr, H.; Bouos-Laurent, H., Eds.; Elsevier: Amsterdam, 1990 (b) Emmelius, M.; Pawlowski, G.; Vollman, H. W. Angew. Chem. Int. Ed. Engl **1989**, 28, 1445.
- (11) Colton, R.; Scollary, G. R. Aust. J. Chem. **1968**, 21, 1427.
- (12) Newton, W. E.; Corbin, J. L.; McDonald, J. W. J. Chem. Dalton Trans. **1974**, 1044.
- (13) Newton, W. E.; Corbin, J. L.; Bravard, D. C.; Searles, J. E.; McDonald, J. W. Inorg. Chem **1974**, 13, 1100.
- (14) Chen, G. J.-J.; McDonald, J. W.; Newton, W. E. Inorg. Chem. **1976**, 15, 2612.
- (15) Moore, F. W.; Larson, M. L. Inorg. Chem. **1967**, 6, 998.
- (16) Binsch, G. Topics Stereochem. **1968**, 3, 97.
- (17) Binsch, G. in Dynamic Nuclear Magnetic Resonance Spectroscopy, Jackman, L. M.; Cotton, F. A., Eds.; Academic Press: New York, 1975, Chap. 3.
- (18) Glasstone, S.; Laidler, K. J.; Eyring, H. The Theory of Rate Processes, McGraw-Hill: New York, 1941; p. 195.
- (19) Shanan-Atidi, H.; Bar-Eli, K. H. J. Phys. Chem. **1970**, 74, 961.
- (20) Barral, R.; Bocard, C.; Série de Roch, I.; Sajus, L.; Tetrahedron Lett. **1972**, 1693.
- (21) Matsuda, T.; Tanaka, K.; Tanaka, T. Inorg. Chem. **1979**, 18, 454.
- (22) Tanaka, T.; Tanaka, K.; Matsuda, T.; Hashi, K. in Ref. 1d, p. 361.
- (23) The seven coordinate Mo in Scheme III is drawn with a pentagonal bipyramidal geometry for convenience - capped octahedral or capped trigonal prismatic geometries are just as plausible, but we have no data on which to prefer any of the common seven

coordinate geometries.<sup>24</sup> The actual geometry of this Mo in the transition state is relatively unimportant since the mechanism in Scheme III places no stereodynamic restrictions on this geometry.

- (24) Kepert, D. L. Prog. Inorg. Chem. 1979, 25, 41.
- (25) (a) Knox, J. R.; Prout, C. K. Acta Crystallagr. B 1969, B25, 1857. (b) Delbaere, L. T. J.; Prout, C. K. J. Chem. Soc. Chem. Commun. 1971, 162. (c) Drew, M.G.B.; Kay, A. J. Chem. Soc. A 1971, 1846. (d) Ricard, L.; Martin, C.; Wiest, R.; Weiss, R. Inorg. Chem. 1975, 14, 2300. (e) Dance, I. G.; Wedd, A. G.; Boyd, I. W. Aust. J. Chem. 1978, 31, 519. (f) Cotton, F. A.; Morehouse, S. M. Inorg. Chem. 1965, 4, 1377. (g) Moynihan, K. J.; Boorman, P. M.; Ball, J. M.; Patel, V. O.; Kerr, K. A. Acta Crystallogr. B 1982, 38, 2258. (h) Cotton, F. A.; Ilsley, W. H. Inorg. Chim. Acta 1982, 59, 213. (i) Wieghardt, K.; Hahn, M.; Swiridoff, W.; Weiss, J. Angew. Chem. Int. Ed. Engl. 1983, 22, 491. (j) Beck, J.; Hiller, W.; Schweda, E.; Strähle, J. Z. Naturforsch. B 1984, 39, 1110.



**Figure 1.** Variable temperature  $^{13}\text{C}$  NMR spectra of  $[\text{Mo}_2\text{O}_3(\text{S}_2^{13}\text{CN}(\text{CH}_2\text{Ph})_2)_4]$  from 220 to 305 K in  $\text{CD}_2\text{Cl}_2$ .

**Figure 2.** Molecular structure of  $[\text{Mo}_2\text{O}_3(\text{S}_2\text{CN}(\text{CH}_2\text{Ph})_2)_4]$  (40% probability ellipsoids). Atoms with an "a" subscript are symmetry generated by inversion through the bridging oxygen.

**Figure 3.** Variable temperature  $^{13}\text{C}$  NMR spectra of  $[\text{Mo}_2\text{O}_3(\text{S}_2^{13}\text{COEt})_4]$  from 230 to 325 K in  $\text{CDCl}_3$ .

**Figure 4.** Variable temperature  $^{13}\text{C}$  NMR spectra of  $[\text{Mo}_2\text{O}_3(\text{S}_2^{13}\text{CO}^i\text{Pr})_4]$  from 230 to 325 K in  $\text{CDCl}_3$ .

**Figure 5.** Molecular structure of  $[\text{Mo}_2\text{O}_3(\text{S}_2\text{CO}^i\text{Pr})_4]$  (40% probability ellipsoids). Atoms with an "a" subscript are symmetry generated by rotation about the two-fold axis.

**Table I.** Summary of Crystal Data, Data Collection, and Refinement Parameters for  $[\text{Mo}_2\text{O}_3\{\text{S}_2\text{CN}(\text{CH}_2\text{Ph})_2\}_2] \cdot 2\text{CH}_2\text{ClCH}_2\text{Cl}$  (**1**· $2\text{CH}_2\text{ClCH}_2\text{Cl}$ ) and  $[\text{Mo}_2\text{O}_3(\text{S}_2\text{CO}^i\text{Pr})_4 \cdot \text{C}_6\text{H}_5\text{CH}_3]$  (**5**· $\text{C}_6\text{H}_5\text{CH}_3$ ).

	<b>1</b>	<b>5</b>
Crystal Data		
formula	$\text{C}_{62}\text{H}_{60}\text{Cl}_4\text{N}_4\text{O}_3\text{S}_8\text{Mo}_2$	$\text{C}_{23}\text{H}_{36}\text{O}_7\text{S}_8\text{Mo}_2$
crystal system	monoclinic	monoclinic
space group	$P 2_1/n$	$C2/c$
$a$ , Å	11.604(4)	25.508(5)
$b$ , Å	21.81(2)	9.659(2)
$c$ , Å	13.85(1)	14.986(4)
$\beta$ , deg	99.90(2)	101.96(2)
$V$ , Å <sup>3</sup>	3453(4)	3613(1)
$Z$	2	4
$\rho$ (calcd), g cm <sup>-3</sup>	1.469	1.605

Data Collection		
$\mu$ , cm <sup>-1</sup>	8.1	11.9
temp, °C	24	24
cryst dims, mm	0.22x0.26x0.34	0.31x0.31x0.36
radiation	Mo K $\alpha$ ( $\lambda$ = 0.71073 Å), graphite-monochromated	
diffractometer	Siemens R3m/V	
scan speed, deg min <sup>-1</sup>	variable, 5-20	variable, 4-14
2 $\theta$ scan range, deg	4<2 $\theta$ <50	4<2 $\theta$ <48
scan technique	$\theta$ -2 $\theta$	$\omega$
data collected	$\pm h$ , $+k$ , $+l$	$+h$ , $+k$ , $\pm l$
weighting factor, g	0.005	0.005
unique data	6094 (6703 read)	5270 (5672 read)
unique data with Fo>6 (Fo)	3654	2818
std rflns	3/197	3/197

Agreement Factors		
R(F), %	4.37	5.52
wR(F), %	6.77	7.63
GOF	0.82	0.87
maximum peak, e Å <sup>-3</sup>	0.54	1.07
data/parameter	9.5:1	16.1:1
$\Delta/\sigma$	0.016	0.029

**Table II.** Fractional Atomic Coordinates ( $\times 10^4$ ) and Equivalent Isotropic DisplacementCoefficients<sup>a</sup> ( $\text{\AA} \times 10^3$ ) for  $[\text{Mo}_2\text{O}_3\{\text{S}_2\text{CN}(\text{CH}_2\text{Ph})_2\}_4]$ .

	x	y	z	U(eq)
Mo	1432(1)	9874(1)	4596(1)	35(1)
S(1)	1620(1)	10948(1)	4022(1)	39(1)
S(2)	2244(2)	10655(1)	6079(1)	42(1)
S(3)	1805(1)	9017(1)	5743(1)	44(1)
S(4)	3564(1)	9610(1)	4831(1)	41(1)
O(1)	0	10000	5000	48(2)
O(2)	1092(4)	9619(2)	3439(3)	56(2)
N(1)	2377(4)	11791(2)	5390(4)	39(2)
N(2)	4109(4)	8819(2)	6318(4)	38(2)
C(1)	2119(5)	11207(3)	5209(4)	34(2)
C(2)	2221(6)	12269(3)	4616(5)	45(2)
C(3)	2841(6)	12012(3)	6385(5)	49(2)
C(4)	3284(5)	9102(3)	5699(5)	36(2)
C(5)	3843(6)	8400(3)	7072(5)	45(2)
C(6)	5374(5)	8950(3)	6355(5)	40(2)
C(11)	1260(8)	13278(3)	4936(6)	63(3)
C(12)	282(10)	13624(4)	4950(7)	81(4)
C(13)	-793(10)	13392(5)	4650(8)	89(4)
C(14)	-925(8)	12776(5)	4375(7)	84(4)
C(15)	57(7)	12423(4)	4381(6)	60(3)
C(16)	1160(6)	12662(3)	4629(5)	47(2)
C(21)	4511(6)	12750(3)	6715(6)	59(3)
C(22)	5695(7)	12883(4)	6843(7)	71(3)
C(23)	6486(7)	12427(4)	6816(6)	69(3)
C(24)	6132(8)	11837(4)	6625(7)	71(3)
C(25)	4953(7)	11713(3)	6472(6)	63(3)
C(26)	4121(6)	12160(3)	6519(5)	47(2)
C(31)	4322(8)	7480(4)	6110(6)	65(3)
C(32)	4781(10)	6910(4)	6062(7)	84(4)
C(33)	5290(9)	6605(4)	6899(9)	85(4)
C(34)	5336(8)	6886(4)	7772(8)	77(4)
C(35)	4893(6)	7468(3)	7830(6)	54(3)
C(36)	4373(5)	7769(3)	7006(5)	43(2)
C(41)	5433(8)	9933(4)	7313(6)	61(3)
C(42)	5898(9)	10291(5)	8099(6)	82(4)
C(43)	6771(10)	10064(6)	8778(7)	90(4)
C(44)	7210(8)	9493(6)	8718(6)	88(4)
C(45)	6738(6)	9117(4)	7933(6)	63(3)
C(46)	5856(5)	9343(3)	7222(5)	43(2)
Cl(1)	9390(2)	10723(1)	10533(2)	92(1)
Cl(2)	7238(3)	10183(2)	11608(2)	135(2)
C(51)	9501(11)	10245(7)	11565(11)	154(7)
C(52)	8690(12)	9954(9)	11793(11)	197(10)

<sup>a</sup>Equivalent isotropic U defined as one third of the trace of the orthogonalized  $U_{ij}$  tensor

**Table III.** Selected Bond Lengths (Å) within [Mo<sub>2</sub>O<sub>3</sub>{S<sub>2</sub>CN(CH<sub>2</sub>Ph)<sub>2</sub>}<sub>4</sub>] (**1**).

Mo-S(1)	2.495 (3)	Mo-S(2)	2.710 (3)
Mo-S(3)	2.444 (3)	Mo-S(4)	2.506 (3)
Mo-O(1)	1.863 (2)	Mo-O(2)	1.677 (5)
S(1)-C(1)	1.740 (6)	S(2)-C(1)	1.692 (6)
S(3)-C(4)	1.738 (6)	S(4)-C(4)	1.706 (7)
N(1)-C(2)	1.483 (8)	N(1)-C(1)	1.323 (8)
N(2)-C(4)	1.323 (7)	N(1)-C(3)	1.471 (8)
N(2)-C(6)	1.487 (8)	N(2)-C(5)	1.460 (9)

**Table IV.** Selected Bond angles (°) within  $[\text{Mo}_2\text{O}_3\{\text{S}_2\text{CN}(\text{CH}_2\text{Ph})_2\}_4]$  **1**.

S(1)-Mo-S(2)	67.2(1)	S(1)-Mo-S(3)	155.5(1)
S(2)-Mo-S(3)	89.3(1)	S(1)-Mo-S(4)	96.8(1)
S(2)-Mo-S(4)	80.7(1)	S(3)-Mo-S(4)	71.3(1)
S(1)-Mo-O(1)	95.1(1)	S(2)-Mo-O(1)	83.8(1)
S(3)-Mo-O(1)	89.1(1)	S(4)-Mo-O(1)	155.0(1)
S(1)-Mo-O(2)	91.6(2)	S(2)-Mo-O(2)	157.9(2)
S(3)-Mo-O(2)	110.7(2)	S(4)-Mo-O(2)	96.5(2)
O(1)-Mo-O(2)	105.1(2)	Mo-S(1)-C(1)	92.2(2)
Mo-S(2)-C(1)	86.1(2)	Mo-S(3)-C(4)	87.7(2)
Mo-S(4)-C(4)	86.4(2)	Mo-O(1)-MoA	180
C(1)-N(1)-C(2)	122.9(5)	C(1)-N(1)-C(3)	121.8(5)
C(2)-N(1)-C(3)	115.3(5)	C(4)-N(2)-C(5)	122.5(5)
C(4)-N(2)-C(6)	122.2(5)	C(5)-N(2)-C(6)	115.1(5)
S(1)-C(1)-S(2)	114.5(3)	S(1)-C(1)-N(1)	121.4(5)
S(2)-C(1)-N(1)	124.1(5)	S(3)-C(4)-S(4)	113.8(3)
S(3)-C(4)-N(2)	122.4(5)	S(4)-C(4)-N(2)	123.7(5)

**Table V.** Fractional Atomic Coordinates ( $\times 10^4$ ) and Equivalent Isotropic Displacement Coefficients<sup>a</sup> for  $[\text{Mo}_2\text{O}_3(\text{S}_2\text{CO}^i\text{Pr})_4]$ .

	x	y	z	U(eq)
Mo	4250(1)	1060(1)	7311(1)	30(1)
S(1)	4226(1)	2051(2)	5794(1)	41(1)
S(2)	3338(1)	2159(3)	6731(1)	47(1)
S(3)	4200(1)	1083(2)	8959(1)	41(1)
S(4)	4439(1)	3622(2)	8077(1)	36(1)
O(1)	5000	917(8)	7500	37(2)
O(2)	4031(3)	-594(6)	7179(4)	47(2)
O(3)	3275(2)	3255(7)	5125(4)	45(2)
O(4)	4420(2)	3527(5)	9796(3)	38(2)
C(1)	3156(4)	4885(11)	3908(7)	57(3)
C(2)	3478(3)	3608(9)	4285(6)	46(3)
C(3)	3392(5)	2380(11)	3651(7)	73(4)
C(4)	4219(4)	3901(9)	11252(6)	52(3)
C(5)	4407(3)	2835(8)	10676(4)	35(2)
C(6)	4973(4)	2334(11)	11064(6)	57(3)
C(7)	3578(3)	2550(8)	5789(5)	39(2)
C(8)	4359(3)	2812(7)	9029(4)	30(2)

<sup>a</sup>Equivalent isotropic U defined as one third of the trace of the orthogonalized  $U_{ij}$  tensor

Table VI. Selected Bond Lengths (Å) within  $[\text{Mo}_2\text{O}_3(\text{S}_2\text{CO}^i\text{Pr})_4]$  (5)

Mo-S(1).	2.455 (2)	Mo-S(2)	2.540 (2)
Mo-S(3)	2.501 (2)	Mo-S(4)	2.728 (2)
Mo-O(1)	1.878 (1)	Mo-O(2)	1.691 (6)
S(1)-C(7)	1.719 (8)	S(2)-C(7)	1.695 (8)
S(3)-C(8)	1.716 (7)	S(4)-C(8)	1.677 (7)
O(3)-C(7)	1.316 (9)	O(3)-C(2)	1.495 (11)
O(4)-C(8)	1.322 (8)	O(4)-C(5)	1.486 (8)



**Table VII.** Selected Bond Angles (°) within [Mo<sub>2</sub>O<sub>3</sub>(S<sub>2</sub>CO<sup>*i*</sup>Pr)<sub>4</sub>] (**5**)

S(1)-Mo-S(2)	71.0(1)	S(1)-Mo-S(3)	156.2(1)
S(2)-Mo-S(3)	95.9(1)	S(1)-Mo-S(4)	90.3(1)
S(2)-Mo-S(4)	80.5(1)	S(3)-Mo-S(4)	67.5(1)
S(1)-Mo-O(1)	89.9(1)	S(2)-Mo-O(1)	156.0(2)
S(3)-Mo-O(1)	96.3(1)	S(4)-Mo-O(1)	85.3(2)
S(1)-Mo-O(2)	108.4(2)	S(2)-Mo-O(2)	95.6(2)
S(3)-Mo-O(2)	92.3(2)	S(4)-Mo-O(2)	158.6(2)
O(1)-Mo-O(2)	104.4(3)	Mo-S(1)-C(7)	87.3(3)
Mo-S(2)-C(7)	85.1(3)	Mo-S(3)-C(8)	90.5(2)
Mo-S(4)-C(8)	83.9(2)	Mo-O(1)-MoA	171.6(5)
C(2)-O(3)-C(7)	120.2(6)	C(5)-O(4)-C(8)	121.1(5)
S(1)-C(7)-S(2)	116.5(4)	S(1)-C(7)-O(3)	124.1(6)
S(2)-C(7)-O(3)	119.3(6)	S(3)-C(8)-S(4)	118.1(4)
S(3)-C(8)-O(4)	123.0(5)	S(4)-C(8)-O(4)	118.9(5)

**Table VIII.** Barriers to Exchange of Dibenzylthiocarbamate Ligands Trans to Bridging and Terminal Oxo Atoms in  $[\text{Mo}_2\text{O}_3\{\text{S}_2^{13}\text{CN}(\text{CH}_2\text{Ph})_2\}_4]$  (1) in 1,2-Dichloroethane at Various Temperatures: (a) As Determined from  $w_{1/2}$  for the Quaternary Carbon Resonance Below Coalescence; (b) as Determined from  $\Delta\nu$  at Coalescence; (c) as Determined from  $w_{1/2}$  of the Averaged Quaternary Carbon Resonance and  $\Delta\nu$  above Coalescence.

T/K	$w_{1/2}/\text{Hz}$	k/Hz	$\Delta G^\ddagger/\text{kcal}\cdot\text{mole}^{-1}$
(a)			
$240 \pm 0.5$	$4.0 \pm 1$	-----	-----
$245 \pm 0.5$	$8.0 \pm 2$	$12.6 \pm 3$	$13.0 \pm 0.2$
$250 \pm 0.5$	$9.8 \pm 2$	$18.2 \pm 3$	$13.1 \pm 0.2$
$255 \pm 0.5$	$10.6 \pm 2$	$20.7 \pm 3$	$13.3 \pm 0.2$
(b)			
$290 \pm 0.5$	-----	$2,080 \pm 25$	$12.6 \pm 0.3$
(c)			
$320 \pm 0.5$	$90 \pm 9$	$16,000 \pm 1,600$	$12.6 \pm 0.7$
$325 \pm 0.5$	$55 \pm 7$	$27,100 \pm 3,400$	$12.5 \pm 0.1$
$330 \pm 0.5$	$46 \pm 5$	$32,900 \pm 3,600$	$12.6 \pm 0.9$
$335 \pm 0.5$	$37 \pm 2$	$41,900 \pm 5,700$	$12.6 \pm 0.7$

$\Delta\nu = 938 \text{ Hz}$

**Table IX.** Activation Parameters for the Exchange of Bridging and Terminal Oxo Atoms in  $[\text{Mo}_2\text{O}_3\text{L}_4]$  Complexes as Determined by Plots of  $\Delta G^\ddagger$  versus Temperature for Data Obtained from Linewidth Data Above Coalescence.

L	$\Delta G^\ddagger_{295}/\text{kcal}\cdot\text{mole}^{-1}$	$\Delta H^\ddagger/\text{kcal}\cdot\text{mole}^{-1}$	$\Delta S^\ddagger/\text{cal}\cdot\text{K}^{-1}\cdot\text{mole}^{-1}$
$\text{S}_2\text{CN}(\text{CH}_2\text{Ph})_2$	$+12.6 \pm 0.1$	$+11.9 \pm 0.4$	$-2.0 \pm 0.6$
$\text{S}_2\text{COEt}$	$+12.3 \pm 0.1$	$+11.1 \pm 0.3$	$-3.9 \pm 1.2$
$\text{S}_2\text{CO}^i\text{Pr}$	$+12.3 \pm 0.1$	$+12.9 \pm 0.4$	$+1.9 \pm 0.6$

**Table X.** Barrier to Exchange of Ethylxanthate Ligands Trans to Bridging and Terminal Oxo Atoms in  $[\text{Mo}_2\text{O}_3(\text{S}_2^{13}\text{COEt})_4]$  in  $\text{CDCl}_3$  at Various Temperatures : (a) as Determined from  $w_{1/2}$  for the Quaternary Carbon Resonance Below Coalescence; (b) as Determined from  $\Delta\nu$  at Coalescence; (c) as Determined from  $w_{1/2}$  of the Averaged Quaternary Carbon Resonance and  $\Delta\nu$  above Coalescence.

T/K	$w_{1/2}/\text{Hz}$	k/Hz	$\Delta G^\ddagger/\text{kcal}\cdot\text{mole}^{-1}$
(a)			
$230 \pm 0.5$	$7.5 \pm 2$	-----	-----
$250 \pm 0.5$	$13.8 \pm 2$	$19.8 \pm 3$	$13.1 \pm 0.1$
$260 \pm 0.5$	$33.8 \pm 2$	$82.6 \pm 3$	$12.9 \pm 0.1$
$270 \pm 0.5$	$93.8 \pm 2$	$271 \pm 3$	$12.8 \pm 0.1$
$280 \pm 0.5$	$263 \pm 2$	$803 \pm 3$	$12.7 \pm 0.1$
(b)			
$283 \pm 0.5$	-----	$3,020 \pm 20$	$12.1 \pm 0.1$
(c)			
$290 \pm 0.5$	$788 \pm 2$	$3,720 \pm 44$	$12.2 \pm 0.1$
$300 \pm 0.5$	$376 \pm 2$	$7,880 \pm 96$	$12.2 \pm 0.1$
$305 \pm 0.5$	$275 \pm 2$	$10,900 \pm 130$	$12.3 \pm 0.1$
$310 \pm 0.5$	$219 \pm 2$	$13,700 \pm 163$	$12.3 \pm 0.1$
$315 \pm 0.5$	$158 \pm 2$	$19,300 \pm 230$	$12.3 \pm 0.1$
$320 \pm 0.5$	$120 \pm 2$	$25,800 \pm 310$	$12.3 \pm 0.1$
$325 \pm 0.5$	$93.8 \pm 2$	$33,700 \pm 400$	$12.3 \pm 0.1$

$$\Delta\nu = 1,360 \pm 2 \text{ Hz}$$

**Table XI.** Barrier to Exchange of Isopropylxanthate Ligands Trans to Bridging and Terminal Oxo Atoms in  $[\text{Mo}_2\text{O}_3(\text{S}_2^{13}\text{CO}^i\text{Pr})_4]$  in  $\text{CDCl}_3$  at Temperatures : (a) as Determined from  $w_{1/2}$  for the Quaternary Carbon Resonance below Coalescence; (b) as Determined from  $\Delta\nu$  at Coalescence; (c) as Determined from  $w_{1/2}$  of the Averaged Quaternary Carbon Resonance and  $\Delta\nu$  above Coalescence.

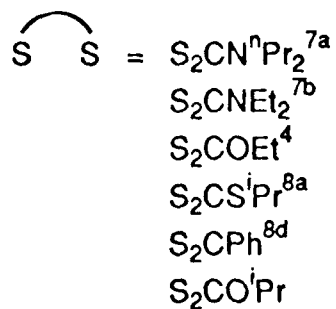
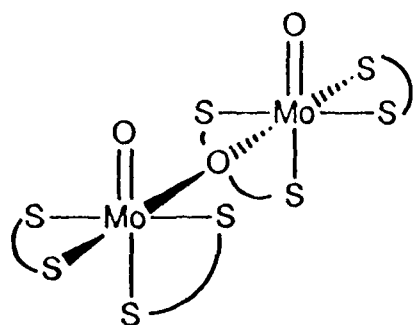
T/K	$w_{1/2}/\text{Hz}$	$k/\text{Hz}$	$\Delta G^\ddagger/\text{kcal}\cdot\text{mole}^{-1}$
(a)			
$225 \pm 0.5$	$6.4 \pm 2$	-----	-----
$230 \pm 0.5$	$8.6 \pm 2$	-----	-----
$240 \pm 0.5$	$11.8 \pm 2$	$17.0 \pm 3$	$12.6 \pm 0.1$
$250 \pm 0.5$	$22.5 \pm 2$	$50.6 \pm 3$	$12.6 \pm 0.1$
$260 \pm 0.5$	$55.7 \pm 2$	$155 \pm 3$	$12.6 \pm 0.1$
$270 \pm 0.5$	$114 \pm 2$	$338 \pm 3$	$12.6 \pm 0.1$
(b)			
$284 \pm 0.5$	-----	$1,750 \pm 20$	$12.4 \pm 0.1$
(c)			
$290 \pm 0.5$	$257 \pm 2$	$3,880 \pm 48$	$12.2 \pm 0.1$
$295 \pm 0.5$	$209 \pm 2$	$4,800 \pm 73$	$12.3 \pm 0.1$
$305 \pm 0.5$	$88.9 \pm 2$	$11,800 \pm 430$	$12.2 \pm 0.1$
$310 \pm 0.5$	$55.7 \pm 2$	$19,700 \pm 600$	$12.1 \pm 0.1$
$315 \pm 0.5$	$53.6 \pm 2$	$20,600 \pm 1300$	$12.3 \pm 0.1$
$325 \pm 0.5$	$34.3 \pm 2$	$34,900 \pm 3700$	$12.3 \pm 0.1$

$$\Delta\nu = 787 \pm 2 \text{ Hz}$$

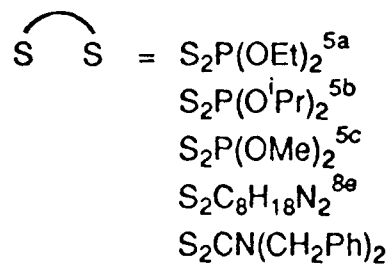
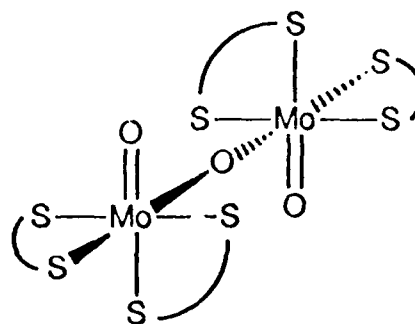
**Table XII.** Free Energies of Activation for the Secondary Exchange Barriers in  $[\text{Mo}_2\text{O}_3\text{L}_4]$  Complexes as Estimated by the Method of Shanan-Atidi and Bar-Eli.\*

L	T/K	$\Delta G^\ddagger_A/\text{kcal}\cdot\text{mole}^{-1}$	$\Delta G^\ddagger_B/\text{kcal}\cdot\text{mole}^{-1}$
$\text{S}_2\text{CN}(\text{CH}_2\text{Ph})_2$	$220 \pm 0.2$	$15.8 \pm 3.2$	$15.3 \pm 3.1$
$\text{S}_2\text{COEt}$	$240 \pm 0.2$	$12.7 \pm 2.5$	$14.2 \pm 2.8$
$\text{S}_2\text{CO}^i\text{Pr}$	$240 \pm 0.2$	$13.0 \pm 2.6$	$14.5 \pm 2.9$

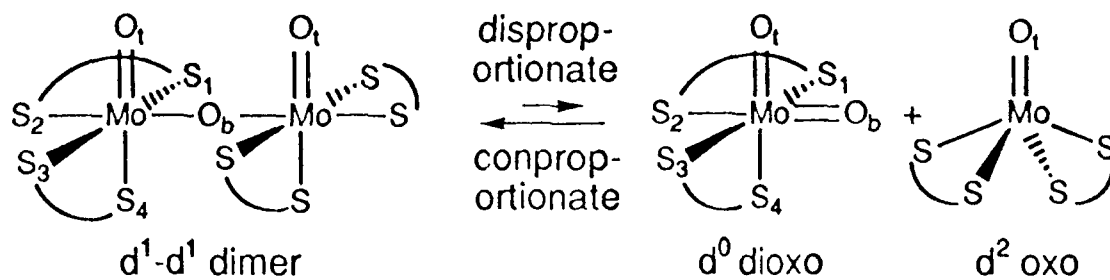
syn complexes:



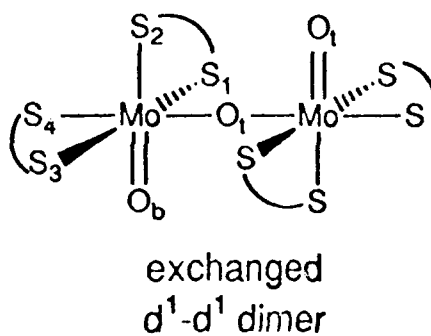
anti complexes:



Schwe I

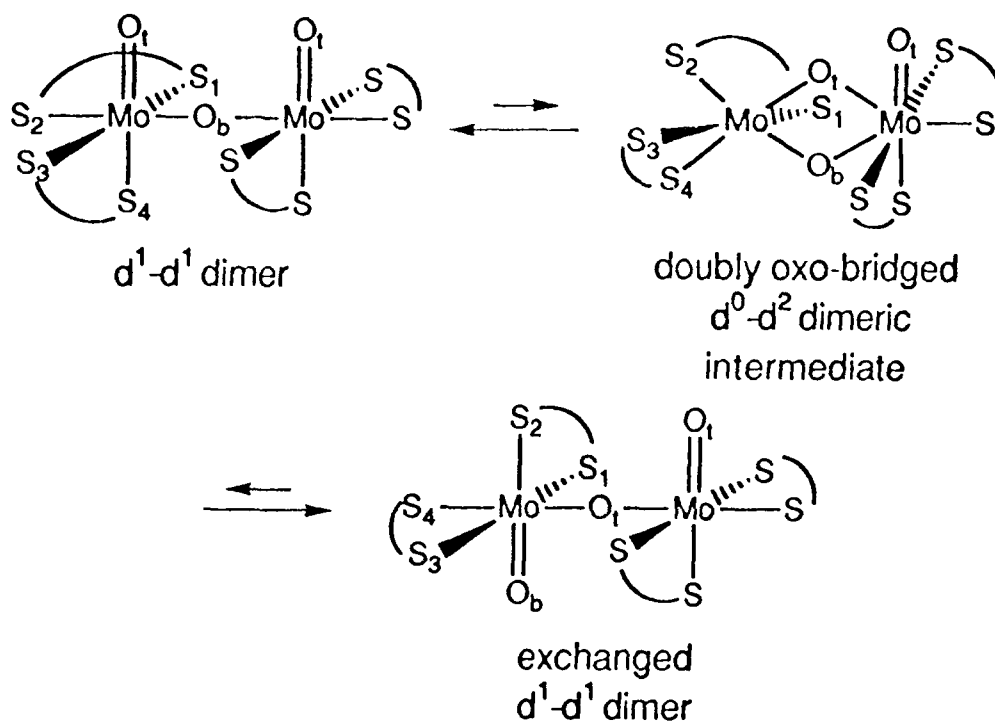


disprop-  
 ortionate  
 $\rightleftharpoons$   
 conprop-  
 ortionate

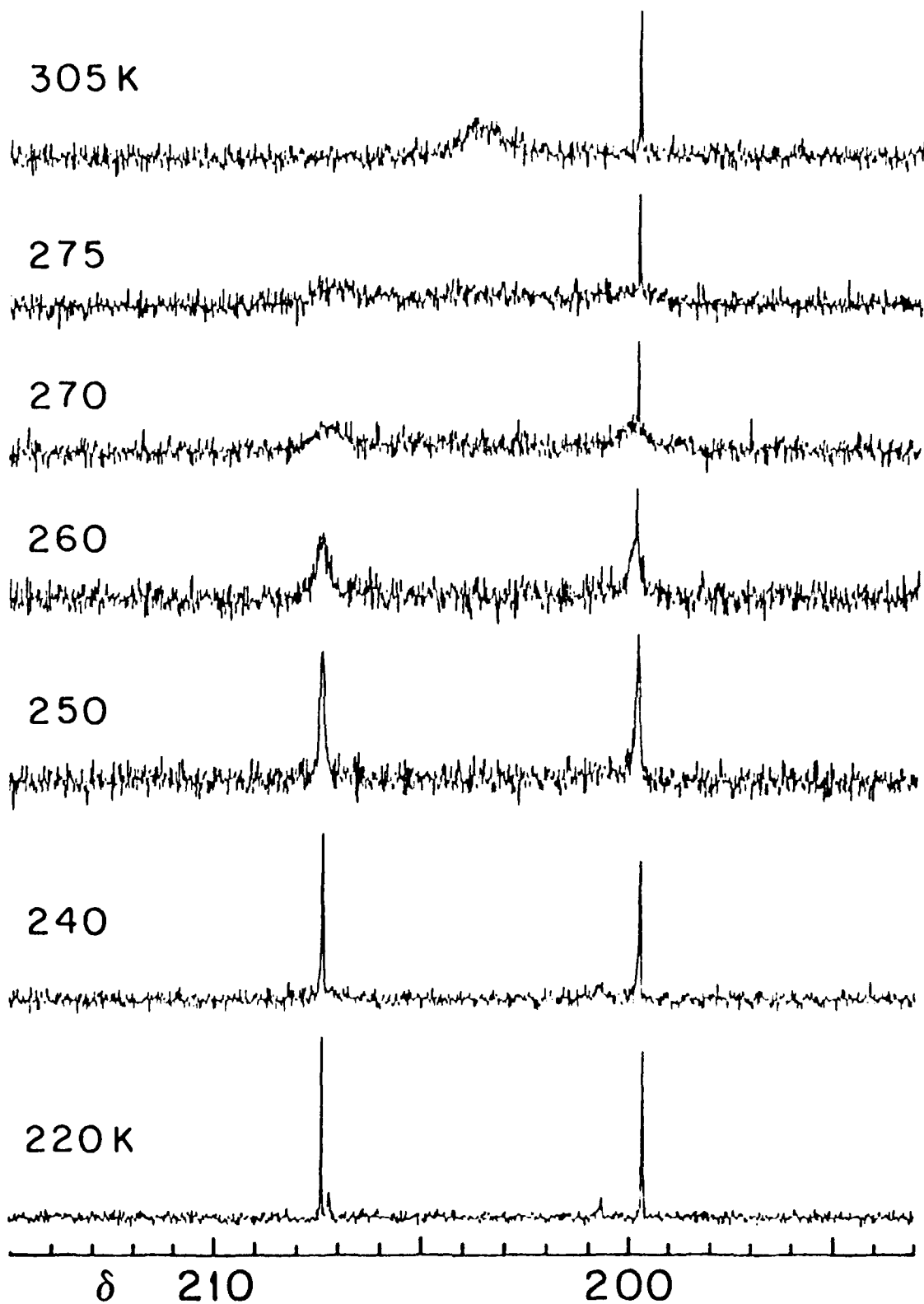


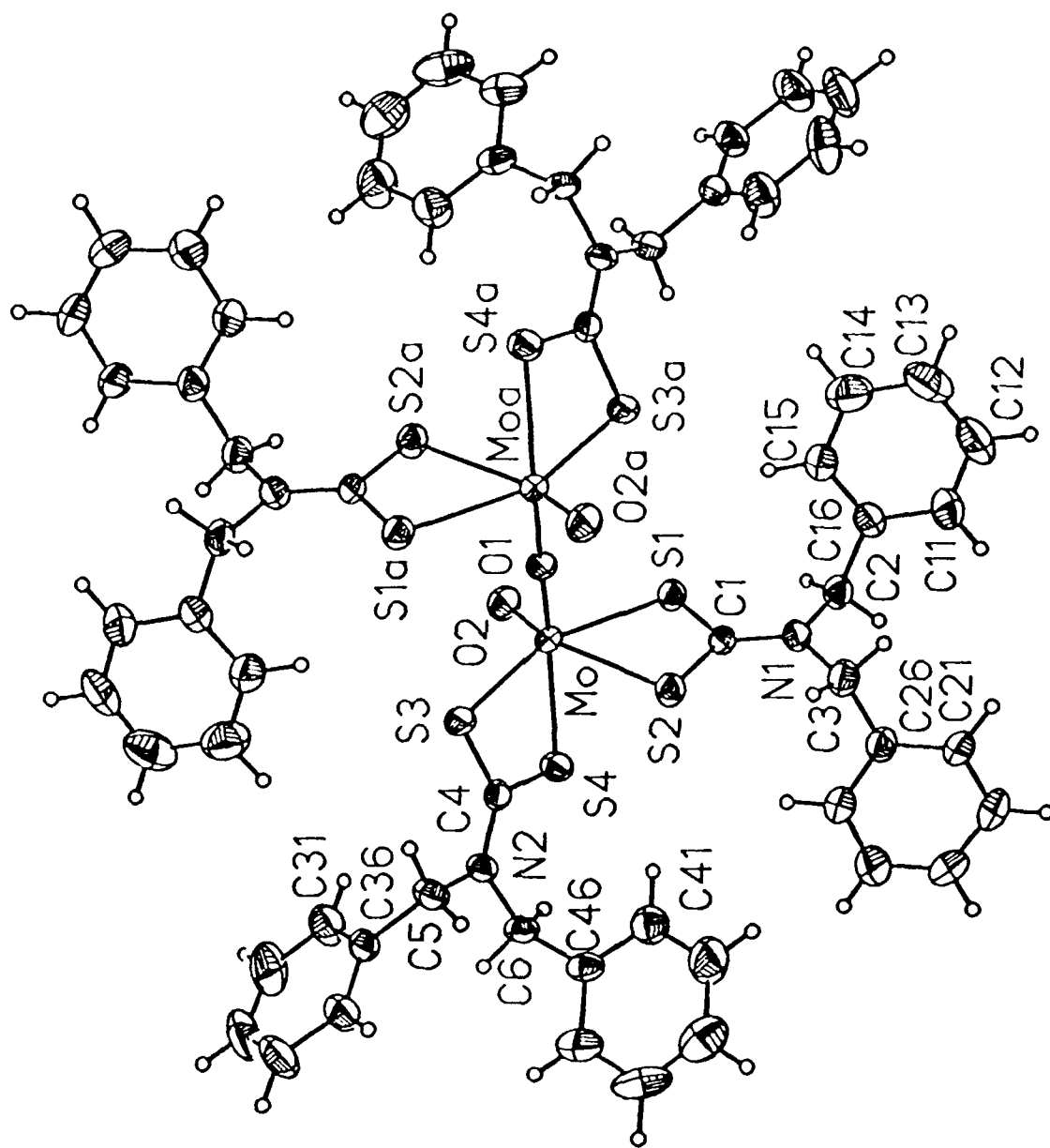
Schwe II

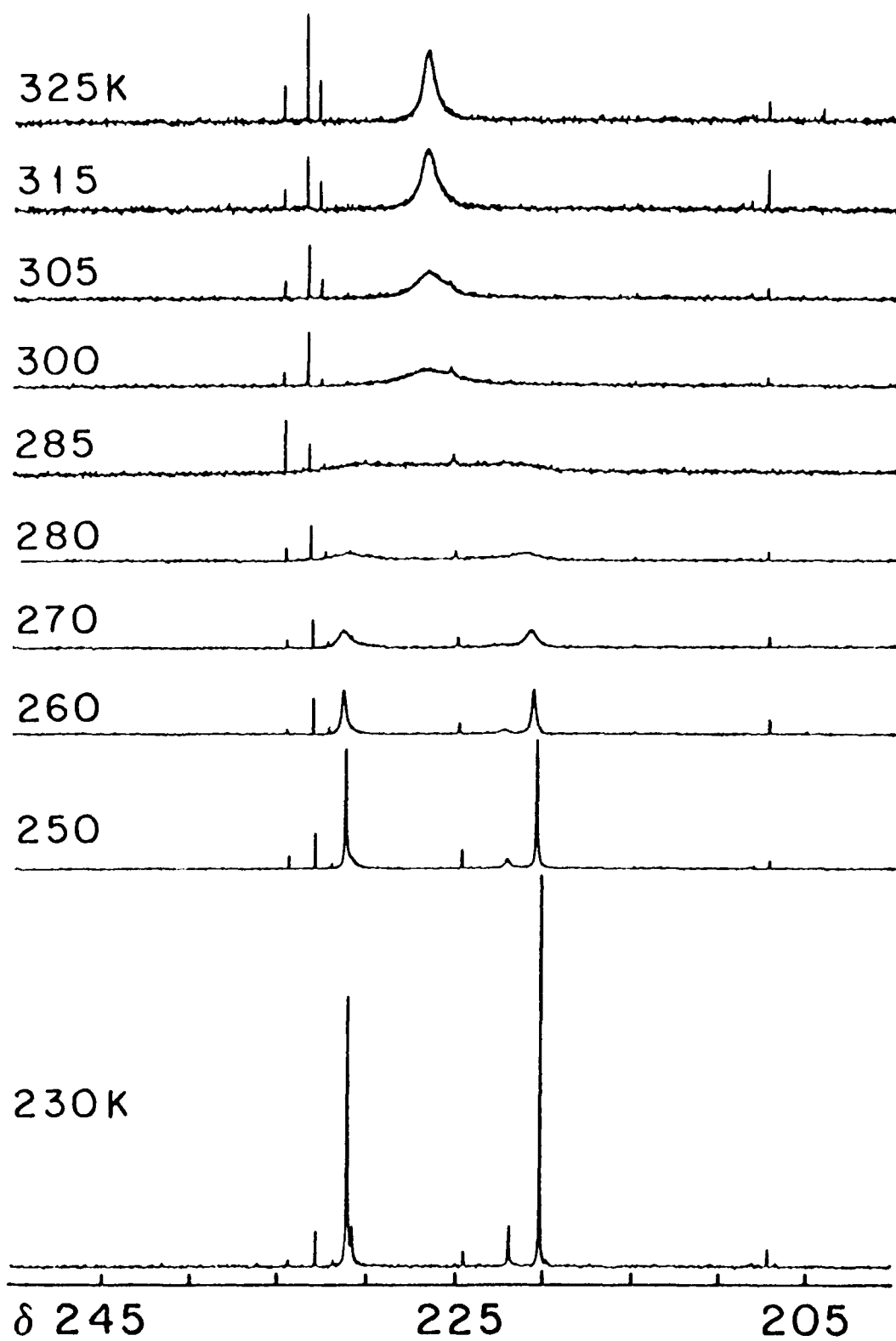


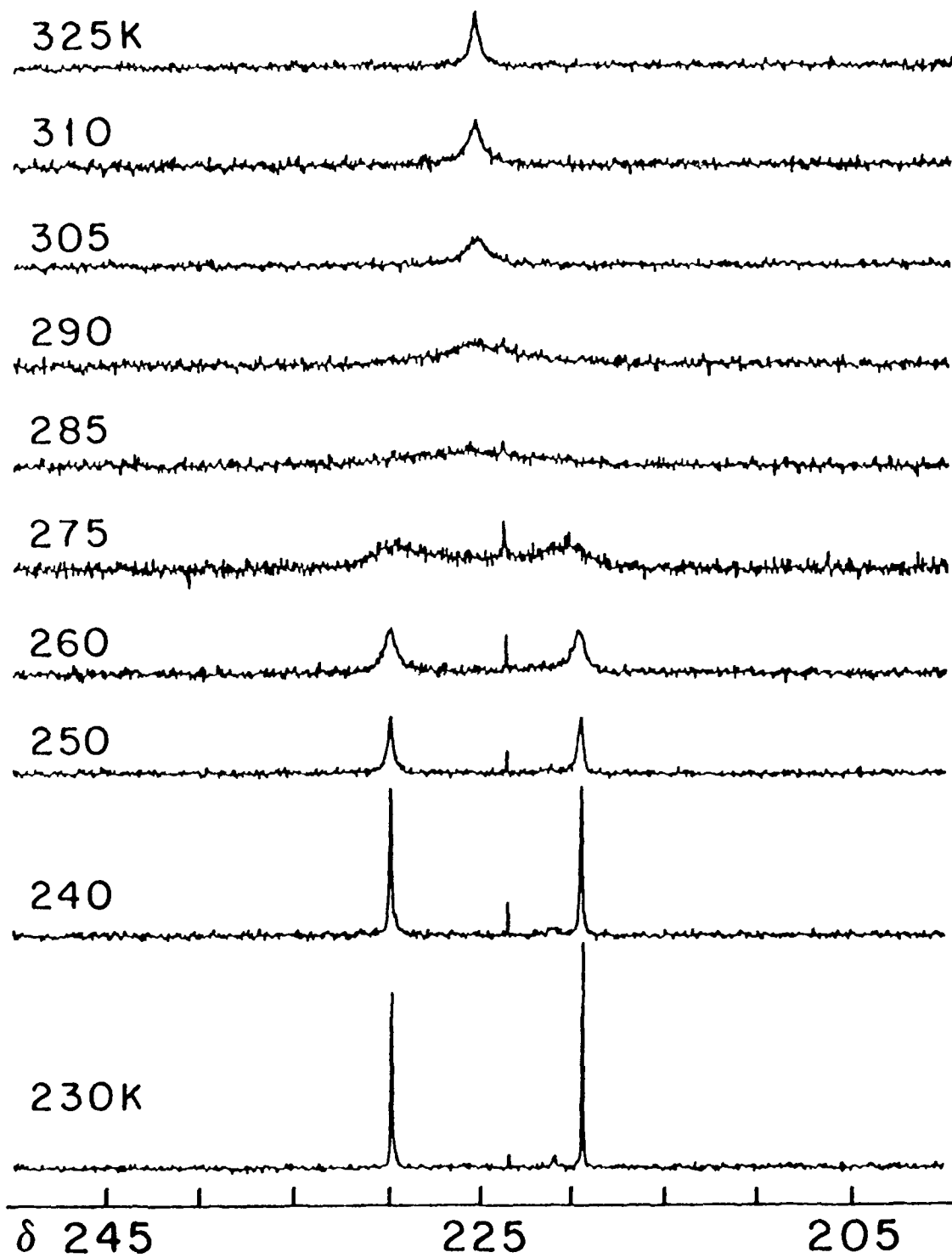


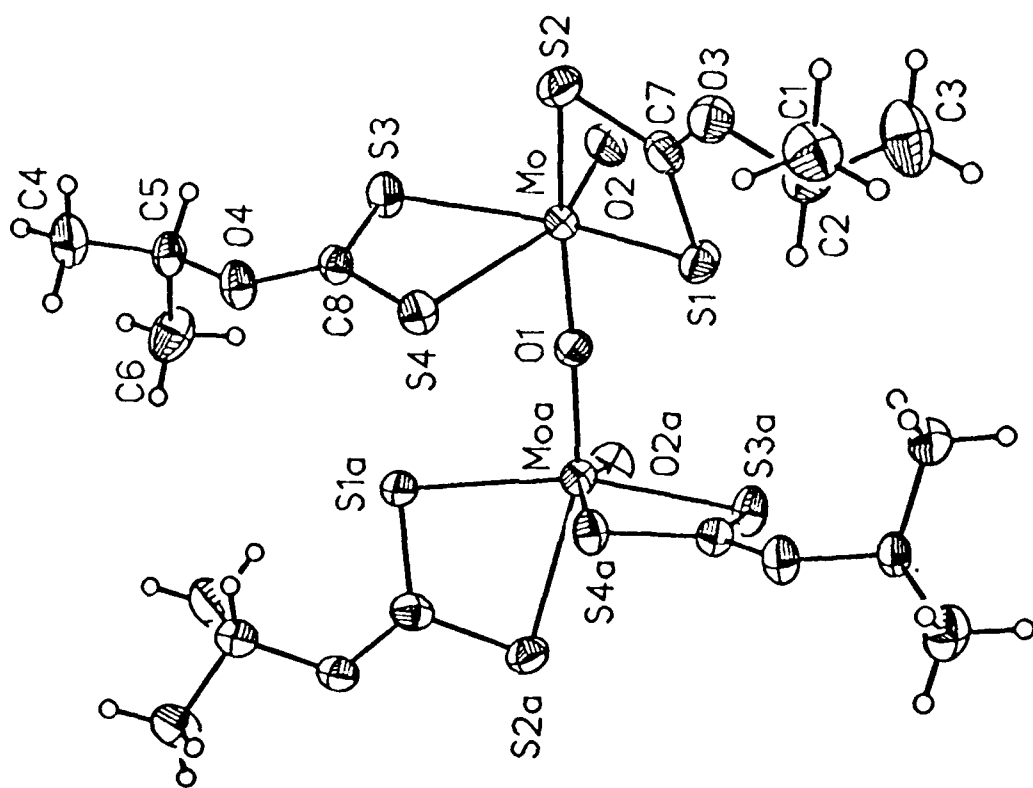
Scheme III











TECHNICAL REPORT DISTRIBUTION LIST - GENERAL

Office of Naval Research (2)\*  
Chemistry Division, Code 1113  
800 North Quincy Street  
Arlington, Virginia 22217-5000

Dr. James S. Murday (1)  
Chemistry Division, Code 6100  
Naval Research Laboratory  
Washington, D.C. 20375-5000

Dr. Robert Green, Director (1)  
Chemistry Division, Code 385  
Naval Air Weapons Center  
Weapons Division  
China Lake, CA 93555-6001

Dr. Elek Lindner (1)  
Naval Command, Control and Ocean  
Surveillance Center  
RDT&E Division  
San Diego, CA 92152-5000

Dr. Bernard E. Douda (1)  
Crane Division  
Naval Surface Warfare Center  
Crane, Indiana 47522-5000

Dr. Richard W. Drisko (1)  
Naval Civil Engineering  
Laboratory  
Code L52  
Port Hueneme, CA 93043

Dr. Harold H. Singerman (1)  
Naval Surface Warfare Center  
Carderock Division Detachment  
Annapolis, MD 21402-1198

Dr. Eugene C. Fischer (1)  
Code 2840  
Naval Surface Warfare Center  
Carderock Division Detachment  
Annapolis, MD 21402-1198

Defense Technical Information  
Center (2)  
Building 5, Cameron Station  
Alexandria, VA 22314

\* Number of copies to forward